International Journal of Solids and Structures 48 (2011) 893–909

Contents lists available at ScienceDirect

International Journal of Solids and Structures

journal homepage: www.elsevier.com/locate/ijsolstr

Thermoelastic problem of steady-state heat flows disturbed by a crack at an arbitrary angle to the graded interfacial zone in bonded materials

Hyung Jip Choi *

School of Mechanical Engineering, Kookmin University, Seoul 136-702, Republic of Korea

ARTICLE INFO

Article history:
Received 4 August 2010
Received in revised form 11 October 2010
Available online 28 November 2010

Keywords:
Bonded materials
Oblique crack
Functionally graded materials
Interfacial zone
Singular integral equations
Heat-flux intensity factors
Thermal-stress intensity factors

ABSTRACT

Plane thermoelasticity solutions are presented for the problem of a crack in bonded materials with a graded interfacial zone. The interfacial zone is treated as a nonhomogeneous interlayer having spatially varying thermoelastic moduli between dissimilar, homogeneous half-planes. The crack is assumed to exist in one of the half-planes at an arbitrary angle to the graded interfacial zone, disturbing uniform steady-state heat flows. The Fourier integral transform method is employed in conjunction with the coordinate transformations of field variables in the basic thermoelasticity equations. Formulation of the current nonisothermal crack problem lends itself to the derivation of two sets of Cauchy-type singular integral equations for heat conduction and thermal stress analyses. The heat-flux intensity factors and the thermal-stress intensity factors are defined and evaluated in order to quantify the singular characters of temperature gradients and thermal stresses, respectively, in the near-tip region. Numerical results include the variations of such crack-tip field intensity factors versus the crack orientation angle for various combinations of material and geometric parameters of the dissimilar media bonded through the thermoelastically graded interfacial zone. The dependence of the near-tip thermoelastic singular field on the degree of crack-surface partial insulation is also addressed.

1. Introduction

The last few decades have witnessed impressive progress in the areas of functionally graded materials, in the light of a number of potential benefits that may stem from the use of such media in a broad range of modern engineering practices, especially in elevated temperature environments. From both the phenomenological and mechanistic viewpoints, this progress can largely be attributed to the tailoring capability to produce gradual variations of thermophysical properties in the spatial domain to accommodate a variety of technological issues (Miyamoto et al., 1999). As a result, the utilization of this new generation of engineered materials in the form of a transitional interlayer in bonded media or as a graded coating deposited on the substrate has become one of the highly innovative and promising applications in coping with various shortcomings that are coupled with the apparent property mismatch inherent in the conventional layered systems (Schulz et al., 2003).

When the damage tolerance is a major concern in structural design with the graded components, the distinct problem area would be to identify crack-tip singularities with the aim of quantifying the effect of material gradations on crack driving forces and other fracture parameters under iso- and nonisothermal loading conditions. A comprehensive review of related earlier studies of focal interest was compiled by Erdogan (1998), underscoring the outstanding features regarding the crack-tip behavior that entails graded, nonhomogeneous properties. The most notable is the near-tip stress field retaining the square-root singularity together with the same angular distributions around the crack tip as those in the homogeneous material, independent of crack orientation, when the spatially varying elastic modulus is continuous and not necessarily differentiable near and at the crack tip. Readers are referred to Eischen (1987) and Jin and Noda (1994a) for the correspondence between the near-tip fields in homogeneous and nonhomogeneous bodies. The standard analysis methodologies can thus be applied to cracks in functionally graded materials such that the influence of material gradations manifests itself through the values of crack driving forces.

Under the isothermal loading condition, a number of additional contributions in the quasi-static crack problems were reported, among others, by Choi (1996, 1997), Paulino et al. (2003), and Chan et al. (2008). In particular, the mixed-mode and anti-plane behavior of a crack at an arbitrary angle to the graded interfacial zone in bonded structures was also investigated by Choi (2001a, 2007a), while the problem of an inclined crack in a graded coating was examined by Long and Delale (2005). Besides, Choi (2001b) tackled the problem of a subsurface crack in a substrate with graded layering under Hertzian contact tractions and Dag and Erdogan (2002) presented the solution for a surface crack in a graded

* Tel.: +82 2 910 4682; fax: +82 2 910 4839.
E-mail address: hjchoi@kookmin.ac.kr

0020-7683/$ - see front matter © 2010 Elsevier Ltd. All rights reserved.
doi:10.1016/j.ijsolstr.2010.11.023

half-plane subjected to a sliding rigid stamp. Most recently, Choi and Paulino (2010) performed the analysis of interfacial cracking in a graded coating/substrate system loaded by a frictional sliding flat punch. The elastodynamic response of a crack in media with the graded properties was further dealt with by Choi (2004, 2006, 2007b) and Lee and Choi (2006).

It is well known that the presence of a crack in a thermally conducting material results in local intensification of temperature gradient in the vicinity of crack tips (Sih, 1965). A thermal disturbance of this type from that in an otherwise unflawed medium may, in turn, induce critical thermal stresses around the crack, leading to a loss of load-carrying capacity and catastrophic failure of structural components through crack propagation. In this respect, taking the spatial variations in both elastic and thermal properties into account, Noda and Jin (1993) and Jin and Noda (1994b) examined the steady-state and transient thermoelastic problems of a crack located parallel to the boundary of a functionally graded material, respectively, whereas Erdogan and Wu (1996) and Jin and Batra (1996) analyzed an edge-cracked strip with graded thermoelastic properties subjected to statically self-equilibrating thermal stresses and sudden cooling, respectively. Subsequently, Choi et al. (1998) studied the thermal shock response of collinear cracks in a layered half-plane with a graded interfacial zone and Fujimoto and Noda (2001) demonstrated how the composition profile of a graded plate affects the crack path under thermal shock. In addition, Choi (2003) provided the mode II thermal stress intensity factors when a uniform heat flow is disturbed by a crack perpendicular to the graded interfacial zone in bonded materials, and Itou (2004) considered the thermal stress problem of a crack in the nonhomogeneous interfacial layer between two dissimilar half-planes. With application to the analysis of a crack in a graded coating, Huang et al. (2004) proposed a multilayered approach by simulating the graded medium as a stack of several sublayers with thermoelastic moduli varying linearly in each sublayer and continuous at the subinterfaces. Moreover, El-Borgi et al. (2003, 2006) and Gharbi et al. (2009) solved, respectively, the thermal loading problems of an interface crack, an embedded crack, and a surface crack in a graded coating. For the interface crack in a graded orthotropic coating/substrate structure, the corresponding thermal-stress intensity factors were evaluated by Chen (2005) and Zhou et al. (2010), in which the crack surfaces were assumed to be perfectly and partially insulated, respectively. It should be noted that various computational models to investigate the thermal fracture behavior of functionally graded materials are available in the literature due to Walters et al. (2004), Yildirim (2006), Kim and Amit (2008) and Dag and Yildirim (2009).

As can be inferred from the aforementioned, the previous attempts undertaken to date for the nonisothermal analyses of cracking with the graded constituents are restricted to relatively simple configurations, for which the symmetries prevail about the crack plane or the normal through the crack center. The present paper is, therefore, devoted to the plane thermoelasticity problem of a crack at an arbitrary angle to the graded interfacial zone in bonded media under steady-state heat flows. The interfacial zone is treated as a nonhomogeneous interlayer with continuous variations of thermoelastic moduli between dissimilar, homogeneous half-planes. In formulating the crack problem, the Fourier integral transform method is employed in conjunction with the coordinate transformations of basic field variables in thermoelasticity. Two sets of Cauchy-type singular integral equations are derived for heat conduction and thermal stresses in the bonded system with the oblique crack. With a view to quantifying the criticality of thermally-induced singular behavior in the near-tip region, the hear-flux intensity factors and the thermal-stress intensity factors are defined and evaluated in terms of the solutions to the integral equations. Numerical results are obtained to illustrate the variations of such crack-tip field intensity factors as a function of crack orientation angle for various combinations of thermoelastic and geometric parameters of the bonded materials. The effect of crack-surface partial insulation on the strength of heat flux and thermal stress singularities is also addressed.

2. Problem statement and governing equations

Consider the two homogeneous half-planes bonded through an interfacial zone with the graded properties. As shown in Fig. 1, the bonded system is subjected to steady-state heat flows of temperature gradients, ∇T_x^∞ and ∇T_y^∞, in the horizontal and vertical directions, respectively, and the half-plane on the right-hand side contains an oblique crack disturbing the heat flows. The global geometric coordinates (x,y) and the local crack coordinates (x_1,y_1) are employed, with the relations between the two coordinates given by:

$$x_1 = mx + ny, \quad y_1 = -nx + my, \tag{1a}$$

$$m = \cos\theta, \quad n = \sin\theta, \tag{1b}$$

where the crack orientation angle θ is measured counterclockwise from the x-axis. In the (x_1,y_1) coordinates, the crack of length $2c$ is directed along the line $a < x_1 < b$ and $y_1 = 0$. With its distance from the interfacial zone designated by d, the crack can be aligned from a perpendicular position ($\theta = 0^\circ$) to a parallel or an interfacial one ($\theta = 90^\circ$) in the bonded media. The cracked half-plane, the interlayer, and the uncracked half-plane are distinguished in order from the right-hand side.

Let thermal conductivity coefficients, shear moduli, and thermal expansion coefficients be denoted by k_j, μ_j, and α_j, $j = 1, 2, 3$, respectively, and the interfacial zone be treated as a nonhomogeneous interlayer of thickness h, with the properties approximated based largely on analytical expediency as (Erdogan and Wu, 1996)

$$k_2(x) = k_1 e^{\delta x}, \quad \mu_2(x) = \mu_1 e^{\beta x}, \quad \alpha_2(x) = \alpha_1 e^{\gamma x}, \tag{2}$$

where the material gradation parameters δ, β, and γ are specified to make the continuous transition of the thermoelastic moduli from one half-plane to the other

$$\delta = \frac{1}{h}\ln\left(\frac{k_1}{k_3}\right), \quad \beta = \frac{1}{h}\ln\left(\frac{\mu_1}{\mu_3}\right), \quad \gamma = \frac{1}{h}\ln\left(\frac{\alpha_1}{\alpha_3}\right) \tag{3}$$

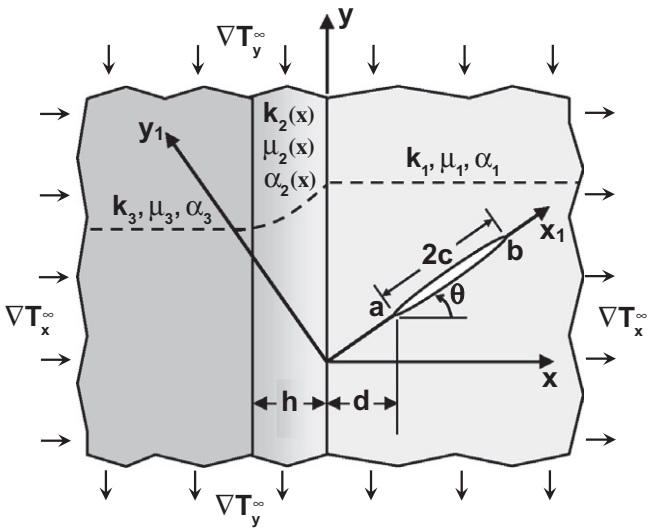

Fig. 1. Bonded dissimilar half-planes containing a crack at an arbitrary angle to the graded interfacial zone under steady-state heat flows.

and the Poisson's ratio is taken to be constant as $v_j = v, j = 1, 2, 3$, because its variation within a practical range exerts an insignificant influence on the values of crack driving forces (Choi, 1997).

Now that the bonded system is thermally loaded sufficiently away from the crack, the resultant full-field temperature consists of the temperature distribution $T_{0j}(x,y)$, $j = 1, 2, 3$, in the absence of a crack and the temperature perturbation $\Theta_j(x,y)$, $j = 1, 2, 3$, caused by the presence of the crack as:

$$T_j(x,y) = T_{0j}(x,y) + \Theta_j(x,y); \quad j = 1,2,3, \tag{4}$$

where the thermoelastic singular response in the near-tip region is typified by the nontrivial temperature field so that the formulation hereinafter is thus given in terms of $\Theta_j(x,y)$, $j = 1, 2, 3$.

The heat flux components are written as:

$$q_{jx} = -k_j \frac{\partial \Theta_j}{\partial x}, \quad q_{jy} = -k_j \frac{\partial \Theta_j}{\partial y}; \quad j = 1,2,3 \tag{5}$$

and with $u_{jx}(x,y)$ and $u_{jy}(x,y)$, $j = 1, 2, 3$, being the displacement components in the x- and y-directions, respectively, the Duhamel–Neumann constitutive equations for the plane thermoelasticity are given by Nowinski (1978):

$$\sigma_{jxx} = \frac{\mu_j}{\kappa - 1}\left[(1+\kappa)\frac{\partial u_{jx}}{\partial x} + (3-\kappa)\frac{\partial u_{jy}}{\partial y} - 4\alpha_j^* \Theta_j\right], \tag{6a}$$

$$\sigma_{jyy} = \frac{\mu_j}{\kappa - 1}\left[(1+\kappa)\frac{\partial u_{jy}}{\partial y} + (3-\kappa)\frac{\partial u_{jx}}{\partial x} - 4\alpha_j^* \Theta_j\right], \tag{6b}$$

$$\sigma_{jxy} = \mu_j\left(\frac{\partial u_{jx}}{\partial y} + \frac{\partial u_{jy}}{\partial x}\right); \quad j = 1,2,3, \tag{6c}$$

where the subscript j is the number referred to the constituent, and $\kappa = 3 - 4v, \alpha_j^* = (1+v)\alpha_j$ for plane strain and $\kappa = (3-v)/(1+v)$, $\alpha_j^* = \alpha_j$ for plane stress.

The steady-state heat conduction equations are expressed as:

$$\nabla^2 \Theta_j + \delta \frac{\partial \Theta_j}{\partial x} = 0; \quad j = 1,2,3 \tag{7}$$

and the Navier–Cauchy equations of equilibrium governing the thermoelastic behavior are written as:

$$\nabla^2 u_{jx} + \frac{2}{\kappa - 1}\frac{\partial}{\partial x}\left(\frac{\partial u_{jx}}{\partial x} + \frac{\partial u_{jy}}{\partial y}\right) + \frac{\beta}{\kappa - 1}\left[(1+\kappa)\frac{\partial u_{jx}}{\partial x} + (3-\kappa)\frac{\partial u_{jy}}{\partial y}\right] = \frac{4\alpha_j^* e^{\gamma x}}{\kappa - 1}\left[(\beta+\gamma)\Theta_j + \frac{\partial \Theta_j}{\partial x}\right], \tag{8a}$$

$$\nabla^2 u_{jy} + \frac{2}{\kappa - 1}\frac{\partial}{\partial y}\left(\frac{\partial u_{jx}}{\partial x} + \frac{\partial u_{jy}}{\partial y}\right) + \beta\left(\frac{\partial u_{jy}}{\partial x} + \frac{\partial u_{jx}}{\partial y}\right) = \frac{4\alpha_j^* e^{\gamma x}}{\kappa - 1}\frac{\partial \Theta_j}{\partial y}; \quad j = 1,2,3, \tag{8b}$$

where $\delta \neq 0$, $\beta \neq 0$, $\gamma \neq 0$ for the graded interlayer ($j = 2$) and $\delta = 0$, $\beta = 0$, $\gamma = 0$ for the homogenous half-planes ($j = 1, 3$). Note that $\alpha_2^* = \alpha_1^*$ when $j = 2$.

In the uncoupled, quasi-static thermoelasticity problem at hand, the temperature perturbation is first to be resolved from the heat conduction problem and the ensuing temperature field is then incorporated into the mixed boundary value problem for thermal stresses.

3. Heat conduction analysis

The assumption of perfect thermal contact along the nominal interfaces yields the continuity conditions for temperature and heat fluxes as:

$$\Theta_1(0,y) = \Theta_2(0,y), \quad \Theta_2(-h,y) = \Theta_3(-h,y); \quad |y| < \infty, \tag{9a}$$

$$q_{1x}(0,y) = q_{2x}(0,y), \quad q_{2x}(-h,y) = q_{3x}(-h,y); \quad |y| < \infty, \tag{9b}$$

$$\Theta_1(+\infty,y) = 0, \quad \Theta_3(-\infty,y) = 0; \quad |y| < \infty \tag{9c}$$

and the mixed thermal boundary conditions on the cracked plane are imposed in the (x_1,y_1) coordinates

$$q_{1y_1}(x_1,+0) = q_{1y_1}(x_1,-0); \quad x_1 > 0, \tag{10a}$$

$$\Theta_1(x_1,+0) = \Theta_1(x_1,-0); \quad 0 < x_1 < a,\ x_1 > b, \tag{10b}$$

$$q_{1y_1}(x_1,+0) = k_1\left(m\nabla T_y^\infty + n\nabla T_x^\infty\right) - h_c[\Theta_1(x_1,+0) - \Theta_1(x_1,-0)]; \quad a < x_1 < b, \tag{10c}$$

where h_c is the ratio between local heat flux and local temperature discontinuity across the crack surfaces and termed as the crack-surface heat conductance (Barber, 1976). It is noted that $h_c > 0$ indicates the partial heat flow between the crack surfaces in proportion to the temperature difference, with the limiting case of $h_c = 0$ corresponding to the completely insulated crack.

The state of temperature and heat fluxes in the half-plane with an arbitrarily oriented crack can be expressed as the sum of two parts in the (x,y) coordinates:

$$\Theta_1(x,y) = \Theta_1^{(1)}(x,y) + \Theta_1^{(2)}(x,y), \tag{11a}$$

$$q_{1j}(x,y) = q_{1j}^{(1)}(x,y) + q_{1j}^{(2)}(x,y); \quad j = x,y \tag{11b}$$

or in the (x_1,y_1) coordinates:

$$\Theta_1(x_1,y_1) = \Theta_1^{(1)}(x_1,y_1) + \Theta_1^{(2)}(x_1,y_1), \tag{12a}$$

$$q_{1j}(x_1,y_1) = q_{1j}^{(1)}(x_1,y_1) + q_{1j}^{(2)}(x_1,y_1); \quad j = x_1,y_1, \tag{12b}$$

where the superscript (1) denotes the infinite plane with a crack and the superscript (2) is for the half-plane without the crack.

For the thermal field in the homogeneous full-plane ($\delta = 0$) containing the crack along $a < x_1 < b$ and $y_1 = 0$, the heat conduction equation is solved based on the Fourier integral transform method to give the general solutions for temperatures in the upper ($y_1 > 0$) and lower ($y_1 < 0$) regions, with those for heat fluxes obtained from Eq. (5). Upon fulfilling the thermal equilibrium in Eq. (10a) and defining an auxiliary function to account for the crack-induced temperature disturbance

$$\phi_0(x_1) = \frac{\partial}{\partial x_1}\left[\Theta_1^{(1)}(x_1,+0) - \Theta_1^{(1)}(x_1,-0)\right]; \quad x_1 > 0, \tag{13}$$

the temperature and heat fluxes in the full-plane are derived in the (x_1,y_1) coordinates as:

$$\Theta_1^{(1)}(x_1,y_1) = -\frac{1}{2\pi}\int_a^b \phi_0(t)\tan^{-1}\left(\frac{t-x_1}{y_1}\right)dt, \tag{14a}$$

$$q_{1x_1}^{(1)}(x_1,y_1) = -\frac{k_1}{2\pi}\int_a^b \frac{\phi_0(t)y_1}{(t-x_1)^2 + y_1^2}dt, \tag{14b}$$

$$q_{1y_1}^{(1)}(x_1,y_1) = -\frac{k_1}{2\pi}\int_a^b \frac{\phi_0(t)(t-x_1)}{(t-x_1)^2 + y_1^2}dt, \tag{14c}$$

subjected to the following continuity and single-valuedness conditions outside the crack line:

$$\phi_0(t) = 0; 0 < t < a, t > b \quad \text{and} \quad \int_a^b \phi_0(t)dt = 0. \tag{15a,b}$$

For the second part of the solution, the general expression of the temperature can readily be obtained in the (x,y) coordinates in terms of the Fourier integral as:

$$\Theta_1^{(2)}(x,y) = \frac{1}{2\pi}\int_{-\infty}^{\infty} A e^{-|s|x - isy}ds; \quad x > 0 \tag{16}$$

and those in the graded interlayer ($\delta \neq 0$) and the uncracked half-plane ($\delta = 0$) are also obtainable as:

$$\Theta_2(x,y) = \frac{1}{2\pi}\int_{-\infty}^{\infty}\sum_{j=1}^{2} B_j e^{\lambda_j x - isy} ds; \quad -h < x < 0, \tag{17}$$

$$\Theta_3(x,y) = \frac{1}{2\pi}\int_{-\infty}^{\infty} C e^{|s|x - isy} ds; \quad x < -h, \tag{18}$$

where s is the transform variable, $A(s)$, $B_j(s)$, $j = 1, 2$, and $C(s)$ are arbitrary unknowns, $i = (-1)^{1/2}$, and $\lambda_j(s)$, $j = 1, 2$, are given by:

$$\lambda_1 = -\frac{\delta}{2} + \sqrt{\frac{\delta^2}{4} + s^2}, \quad \lambda_2 = -\frac{\delta}{2} - \sqrt{\frac{\delta^2}{4} + s^2}. \tag{19}$$

The thermal interface continuity conditions, Eqs. (9a) and (9b), can now be applied to determine the four unknowns, $A(s)$, $B_j(s)$, $j = 1, 2$, and $C(s)$, in terms of the auxiliary function ϕ_0, which then remains to be evaluated from the thermal crack-surface condition in Eq. (10c). To this end, the field components for the cracked half-plane in the (x,y) coordinates, Eqs. (11a) and (11b), are employed. The full-plane solutions in Eqs. (14a)–(14c) obtained in the (x_1,y_1) coordinates should thus be transformed to those in the (x,y) coordinates

$$\Theta_1(x,y) = \Theta_1^{(1)}(x_1,y_1) + \Theta_1^{(2)}(x,y), \tag{20a}$$

$$q_{1x}(x,y) = m q_{1x_1}^{(1)}(x_1,y_1) - n q_{1y_1}^{(1)}(x_1,y_1) + q_{1x}^{(2)}(x,y), \tag{20b}$$

where from Eqs. (14) and (16), together with Eqs. (1) and (5), it can be shown that:

$$\Theta_1(x,y) = -\frac{1}{2\pi}\int_a^b \phi_0(t)\tan^{-1}\left(\frac{t-mx-ny}{my-nx}\right)dt + \frac{1}{2\pi}\int_{-\infty}^{\infty} A e^{-|s|x-isy} ds,$$

$$q_{1x}(x,y) = \frac{k_1}{2\pi}\int_a^b \phi_0(t)\left[\frac{nt-y}{x^2+y^2+t^2-2t(mx+ny)}\right]dt + \frac{k_1}{2\pi}\int_{-\infty}^{\infty} A|s| e^{-|s|x-isy} ds \tag{21a, b}$$

and by substituting Eqs. (17), (18) and (21) into Eqs. (9a) and (9b), the unknowns, $A(s)$, $B_j(s)$, $j = 1, 2$, and $C(s)$, can be expressed in terms of the function ϕ_0 as provided in Appendix A.

Subsequently, the heat flux component in the y_1-direction for the cracked half-plane is written from Eq. (12b), with its second part transformed as:

$$q_{1y_1}(x_1,y_1) = q_{1y_1}^{(1)}(x_1,y_1) - n q_{1x}^{(2)}(x,y) + m q_{1y}^{(2)}(x,y), \tag{22a}$$

$$x = m x_1 - n y_1, \quad y = n x_1 + m y_1 \tag{22b}$$

and using Eqs. (5), (14c) and (16), one can obtain the following:

$$2\pi \lim_{y_1 \to +0} \frac{\partial \Theta_1}{\partial y_1}(x_1,y_1) = \int_a^b \frac{\phi_0(t)}{t-x_1}dt + \int_{-\infty}^{\infty} A(n|s| - ims) e^{-(m|s| + ins)x_1} ds; \quad x_1 > 0, \tag{23}$$

where the first term on the right-hand side is the integral with a Cauchy singular kernel.

After making use of the expression $A(s)$ in Eq. (A.1) and applying the crack-surface condition in Eq. (10c), a singular integral equation can be derived for heat conduction

$$\int_a^b \frac{\phi_0(t)}{t-x_1}dt + \int_a^b k_0(x_1,t)\phi_0(t)dt - \frac{2\pi h_c}{k_1}\int_a^{x_1}\phi_0(t)dt = -2\pi\nabla T_\infty; \quad a < x_1 < b, \tag{24}$$

where $k_0(x_1,t)$ is a kernel bounded in the interval $[a,b]$ and ∇T_∞ denotes the equivalent temperature gradient across the crack surfaces

$$k_0(x_1,t) = \int_0^\infty \Lambda_0(s)[m\cos ns(t-x_1) - n\sin ns(t-x_1)]e^{-ms(t+x_1)}ds,$$

$$\nabla T_\infty = m\nabla T_y^\infty + n\nabla T_x^\infty \tag{25a, b}$$

and the function $\Lambda_0(s)$ is written as:

$$\Lambda_0(s) = \frac{\delta\left(e^{-h\sqrt{\delta^2+4s^2}} - 1\right)}{2s\left(e^{-h\sqrt{\delta^2+4s^2}} - 1\right) - \sqrt{\delta^2+4s^2}\left(e^{-h\sqrt{\delta^2+4s^2}} + 1\right)}, \tag{26}$$

which is for the crack oriented perpendicular to the nominal interface.

4. Thermal stress analysis

For the incumbent thermoelasticity problem of bonded media with a graded interlayer, the conditions of displacement continuity and traction equilibrium along the nominal interfaces should be fulfilled as:

$$u_{1x}(0,y) = u_{2x}(0,y), \quad u_{1y}(0,y) = u_{2y}(0,y); \quad |y| < \infty, \tag{27a}$$

$$u_{2x}(-h,y) = u_{3x}(-h,y), \quad u_{2y}(-h,y) = u_{3y}(-h,y); \quad |y| < \infty, \tag{27b}$$

$$\sigma_{1xx}(0,y) = \sigma_{2xx}(0,y), \quad \sigma_{1xy}(0,y) = \sigma_{2xy}(0,y); \quad |y| < \infty, \tag{27c}$$

$$\sigma_{2xx}(-h,y) = \sigma_{3xx}(-h,y), \quad \sigma_{2xy}(-h,y) = \sigma_{3xy}(-h,y); \quad |y| < \infty, \tag{27d}$$

$$u_{1j}(+\infty,y) \to 0, \quad u_{3j}(-\infty,y) = 0; \quad j = x,y, \ |y| < \infty \tag{27e}$$

and the mixed mechanical boundary conditions on the cracked plane are prescribed in the (x_1,y_1) coordinates as:

$$\sigma_{1y_1y_1}(x_1,+0) = \sigma_{1y_1y_1}(x_1,-0), \quad \sigma_{1x_1y_1}(x_1,+0) = \sigma_{1x_1y_1}(x_1,-0); \quad x_1 > 0, \tag{28a}$$

$$u_{1x_1}(x_1,+0) = u_{1x_1}(x_1,-0), \quad u_{1y_1}(x_1,+0) = u_{1y_1}(x_1,-0); \quad 0 < x_1 < a, \ x_1 > b, \tag{28b}$$

$$\sigma_{1y_1y_1}(x_1,+0) = 0, \quad \sigma_{1x_1y_1}(x_1,+0) = 0; \quad a < x_1 < b. \tag{28c}$$

As in the case of prior heat conduction analysis, for the half-plane with an oblique crack, the corresponding state of thermoelastic displacements and stresses can be written as the sum of two parts in the (x,y) coordinates:

$$u_{1i}(x,y) = u_{1i}^{(1)}(x,y) + u_{1i}^{(2)}(x,y); \quad i = x,y, \tag{29a}$$

$$\sigma_{1ij}(x,y) = \sigma_{1ij}^{(1)}(x,y) + \sigma_{1ij}^{(2)}(x,y); \quad i,j = x,y \tag{29b}$$

or in the (x_1,y_1) coordinate system:

$$u_{1i}(x_1,y_1) = u_{1i}^{(1)}(x_1,y_1) + u_{1i}^{(2)}(x_1,y_1); \quad i = x_1,y_1, \tag{30a}$$

$$\sigma_{1ij}(x_1,y_1) = \sigma_{1ij}^{(1)}(x_1,y_1) + \sigma_{1ij}^{(2)}(x_1,y_1); \quad i,j = x_1,y_1, \tag{30b}$$

where the superscripts (1) and (2), respectively, refer to the infinite plane containing a crack and the half-plane without the crack.

In order to find the thermoelastic field components in the homogeneous full-plane ($\delta = 0, \beta = 0, \gamma = 0$) with the crack along

$a < x_1 < b$ and $y_1 = 0$, the general solutions for displacements in the upper ($y_1 > 0$) and lower ($y_1 < 0$) regions are obtained by solving the Navier–Cauchy governing equations in Eqs. (8a) and (8b) and those for stresses are obtainable from the constitutive relations in Eqs. (6a)–(6c). After enforcing the traction equilibrium in Eq. (28a) and introducing two auxiliary functions

$$\phi_1(x_1) = \frac{\partial}{\partial x_1}\left[u^{(1)}_{1y_1}(x_1,+0) - u^{(1)}_{1y_1}(x_1,-0)\right]; \quad x_1 > 0, \tag{31a}$$

$$\phi_2(x_1) = \frac{\partial}{\partial x_1}\left[u^{(1)}_{1x_1}(x_1,+0) - u^{(1)}_{1x_1}(x_1,-0)\right]; \quad x_1 > 0 \tag{31b}$$

and with the use of relevant expressions from the result of heat conduction analysis, the components of thermoelastic displacements and stresses in the full-plane can be derived in the (x_1,y_1) coordinates:

$$\begin{aligned}\pi u^{(1)}_{1x_1}(x_1,y_1) &= \frac{\alpha_1^*}{1+\kappa}\int_a^b \phi_0(t) y_1 \ln\left[(t-x_1)^2+y_1^2\right]^{1/2} dt \\ &+ \frac{1}{1+\kappa}\int_a^b \phi_1(t)\left[\frac{(1-\kappa)}{2}\ln\left[(t-x_1)^2+y_1^2\right]^{1/2} - \frac{y_1^2}{(t-x_1)^2+y_1^2}\right] dt \\ &- \frac{1}{1+\kappa}\int_a^b \phi_2(t)\left[\frac{(1+\kappa)}{2}\tan^{-1}\frac{t-x_1}{y_1} - \frac{(t-x_1)y_1}{(t-x_1)^2+y_1^2}\right] dt,\end{aligned} \tag{32a}$$

$$\begin{aligned}\pi u^{(1)}_{1y_1}(x_1,y_1) &= \frac{\alpha_1^*}{1+\kappa}\int_a^b \phi_0(t)\left[(t-x_1)\left\{1-\ln\left[(t-x_1)^2+y_1^2\right]^{1/2}\right\}\right. \\ &\left. - 2y_1\tan^{-1}\frac{t-x_1}{y_1}\right] dt - \frac{1}{1+\kappa}\int_a^b \phi_1(t)\left[\frac{(1+\kappa)}{2}\tan^{-1}\frac{t-x_1}{y_1}\right. \\ &\left. + \frac{(t-x_1)y_1}{(t-x_1)^2+y_1^2}\right] dt - \frac{1}{1+\kappa}\int_a^b \phi_2(t)\left[\frac{(1-\kappa)}{2}\ln\left[(t-x_1)^2+y_1^2\right]^{1/2}\right. \\ &\left. + \frac{y_1^2}{(t-x_1)^2+y_1^2}\right] dt,\end{aligned} \tag{32b}$$

$$\begin{aligned}\frac{\pi(1+\kappa)}{2\mu_1}\sigma^{(1)}_{1x_1x_1}(x_1,y_1) &= \alpha_1^*\int_a^b \phi_0(t)\left[2\tan^{-1}\frac{t-x_1}{y_1} - \frac{(t-x_1)y_1}{(t-x_1)^2+y_1^2}\right] dt \\ &+ \int_a^b \phi_1(t)\left[\frac{t-x_1}{(t-x_1)^2+y_1^2} - \frac{2(t-x_1)y_1^2}{\left[(t-x_1)^2+y_1^2\right]^2}\right] dt \\ &+ \int_a^b \phi_2(t) y_1\left[\frac{2}{(t-x_1)^2+y_1^2} + \frac{(t-x_1)^2-y_1^2}{\left[(t-x_1)^2+y_1^2\right]^2}\right] dt,\end{aligned} \tag{32c}$$

$$\begin{aligned}\frac{\pi(1+\kappa)}{2\mu_1}\sigma^{(1)}_{1y_1y_1}(x_1,y_1) &= \alpha_1^*\int_a^b \phi_0(t)\frac{(t-x_1)y_1}{(t-x_1)^2+y_1^2} dt \\ &+ \int_a^b \phi_1(t)\left[\frac{t-x_1}{(t-x_1)^2+y_1^2} + \frac{2(t-x_1)y_1^2}{\left[(t-x_1)^2+y_1^2\right]^2}\right] dt \\ &- \int_a^b \phi_2(t) y_1\frac{(t-x_1)^2-y_1^2}{\left[(t-x_1)^2+y_1^2\right]^2} dt,\end{aligned} \tag{32d}$$

$$\begin{aligned}\frac{\pi(1+\kappa)}{2\mu_1}\sigma^{(1)}_{1x_1y_1}(x_1,y_1) &= \alpha_1^*\int_a^b \phi_0(t)\left[\frac{y_1^2}{(t-x_1)^2+y_1^2} + \ln\left[(t-x_1)^2+y_1^2\right]^{1/2}\right] dt \\ &- \int_a^b \phi_1(t) y_1\frac{(t-x_1)^2-y_1^2}{\left[(t-x_1)^2+y_1^2\right]^2} dt \\ &+ \int_a^b \phi_2(t)\left[\frac{t-x_1}{(t-x_1)^2+y_1^2} - \frac{2(t-x_1)y_1^2}{\left[(t-x_1)^2+y_1^2\right]^2}\right] dt,\end{aligned} \tag{32e}$$

where the functions ϕ_j, $j = 1, 2$, should satisfy the conditions of continuity and single-valuedness as:

$$\phi_j(t) = 0; \quad 0 < t < a,\ t > b \quad \text{and} \quad \int_a^b \phi_j(t)dt = 0; \quad j = 1,2. \tag{33a,b}$$

For the second part, the general solutions for the displacement components are readily obtainable in the (x,y) coordinates in terms of the Fourier integrals

$$\begin{aligned}u^{(2)}_{1x}(x,y) &= -\frac{i}{2\pi}\int_{-\infty}^{\infty}\frac{s}{|s|}\left[F_1 + F_2\left(x+\frac{\kappa}{|s|}\right)\right]e^{-|s|x-isy} ds \\ &+ \frac{\alpha_1^*}{\pi(1+\kappa)}\int_{-\infty}^{\infty} A\left(x-\frac{1}{|s|}\right)e^{-|s|x-isy} ds,\end{aligned} \tag{34a}$$

$$\begin{aligned}u^{(2)}_{1y}(x,y) &= \frac{1}{2\pi}\int_{-\infty}^{\infty}(F_1 + F_2 x)e^{-|s|x-isy} ds \\ &+ \frac{\alpha_1^* i}{\pi(1+\kappa)}\int_{-\infty}^{\infty} A\frac{s}{|s|}xe^{-|s|x-isy} ds; \quad x > 0,\end{aligned} \tag{34b}$$

where $F_j(s)$, $j = 1, 2$, are arbitrary unknowns.

The general expressions of the displacements in the graded interlayer ($\delta \neq 0, \beta \neq 0, \gamma \neq 0$) can be also obtained as:

$$\begin{aligned}u_{2x}(x,y) &= -\frac{i}{2\pi}\int_{-\infty}^{\infty}\sum_{j=1}^{4} G_j m_j e^{n_j x-isy} ds \\ &- \frac{2\alpha_1^* e^{\gamma x}}{\pi(1-\kappa)}\int_{-\infty}^{\infty}\sum_{j=1}^{2} B_j\frac{\Phi_j}{\Delta_j}e^{\lambda_j x-isy} ds,\end{aligned} \tag{35a}$$

$$\begin{aligned}u_{2y}(x,y) &= \frac{1}{2\pi}\int_{-\infty}^{\infty}\sum_{j=1}^{4} G_j e^{n_j x-isy} ds \\ &- \frac{2\alpha_1^* e^{\gamma x} i}{\pi(1-\kappa)}\int_{-\infty}^{\infty}\sum_{j=1}^{2} B_j\frac{\Omega_j}{\Delta_j}e^{\lambda_j x-isy} ds; \quad -h < x < 0,\end{aligned} \tag{35b}$$

where $G_j(s)$, $j = 1,\ldots,4$, are arbitrary unknowns, $n_j(s)$, $j = 1,\ldots,4$, are the roots of the characteristic equation

$$(n^2 + \beta n - s^2)^2 + \left(\frac{3-\kappa}{1+\kappa}\right)\beta^2 s^2 = 0, \tag{36}$$

from which it follows that:

$$n_j = -\frac{\beta}{2} + \sqrt{\frac{\beta^2}{4} + s^2 - i(-1)^j\beta s\left(\frac{3-\kappa}{1+\kappa}\right)^{1/2}}; \quad Re(n_j) > 0,\ j = 1,2, \tag{37a}$$

$$n_j = -\frac{\beta}{2} - \sqrt{\frac{\beta^2}{4} + s^2 + i(-1)^j\beta s\left(\frac{3-\kappa}{1+\kappa}\right)^{1/2}}; \quad Re(n_j) < 0,\ j = 3,4 \tag{37b}$$

and $m_j(s)$, $j = 1,\ldots,4$, are given for each root as:

$$m_j = \frac{(1-\kappa)(n_j^2+\beta n_j)+(1+\kappa)s^2}{[(1-\kappa)\beta-2n_j]s}. \tag{38}$$

Moreover, the thermoelastic constants, $\Phi_j(s)$, $\Omega_j(s)$, and $\Delta_j(s)$, $j = 1, 2$, in the particular solutions in Eqs. (35a) and (35b) are defined as:

$$\Phi_j = (\beta+\gamma+\lambda_j)\left[\frac{4\kappa s^2}{1-\kappa^2}-\left(\frac{1-\kappa}{1+\kappa}\right)P_j\right]+Q_j s^2, \tag{39a}$$

$$\Omega_j = s(\beta+\gamma+\lambda_j)\left[Q_j+2\beta\left(\frac{2-\kappa}{1-\kappa}\right)\right]-P_j s, \tag{39b}$$

$$\Delta_j = \left[\frac{4\kappa s^2}{1-\kappa^2}-\left(\frac{1-\kappa}{1+\kappa}\right)P_j\right]P_j+\left[Q_j+2\beta\left(\frac{2-\kappa}{1-\kappa}\right)\right]Q_j s^2 \tag{39c}$$

in which $P_j(s)$ and $Q_j(s)$, $j = 1, 2$, are given by:

$$P_j = -\left(\frac{1+\kappa}{1-\kappa}\right)(\gamma+\lambda_j)(\beta+\gamma+\lambda_j)-s^2, \tag{40a}$$

$$Q_j = \frac{\beta(\kappa-3)-2(\gamma+\lambda_j)}{1-\kappa}. \tag{40b}$$

For the uncracked half-plane on the left-hand side ($\delta = 0, \beta = 0$, $\gamma = 0$), the general expressions of the displacement components are written as:

$$u_{3x}(x,y) = \frac{i}{2\pi}\int_{-\infty}^{\infty}\frac{s}{|s|}\left[H_1+H_2\left(x-\frac{\kappa}{|s|}\right)\right]e^{|s|x-isy}ds + \frac{\alpha_3^*}{\pi(1+\kappa)}\int_{-\infty}^{\infty}C\left(x+\frac{1}{|s|}\right)e^{|s|x-isy}ds, \tag{41a}$$

$$u_{3y}(x,y) = \frac{1}{2\pi}\int_{-\infty}^{\infty}(H_1+H_2x)e^{|s|x-isy}ds - \frac{\alpha_3^* i}{\pi(1+\kappa)}\int_{-\infty}^{\infty}C\frac{s}{|s|}xe^{|s|x-isy}ds; \quad x<-h, \tag{41b}$$

where $H_j(s)$, $j = 1, 2$, are arbitrary unknowns.

As can be seen in the above, the general solutions involved in the thermal stress analysis have a total of eight unknowns, $F_j(s)$, $j = 1, 2$, $G_j(s)$, $j = 1,\ldots,4$, and $H_j(s)$, $j = 1, 2$. The direct application of interface conditions for the displacements and tractions, Eqs. (27a)–(27d), would lead to a system of algebraic equations to be solved for these unknowns in terms of ϕ_j, $j = 1, 2$, and ϕ_0 as well. In what follows, as a judicious way of accomplishing such a routine procedure, the transfer matrix approach (Bahar, 1972) is exploited, the result of which is to be utilized in deriving the integral equations for thermal stresses.

4.1. Application of interface conditions for thermal stresses

In order to apply the interface conditions in Eqs. (27a)–(27d), the field components for the cracked half-plane in Eqs. (29a) and (29b) as written in the (x,y) coordinates are employed, followed by the transformation of full-plane solutions in Eqs. (32a)–(32e) obtained in the (x_1,y_1) coordinates to those in the (x,y) coordinates and the use of Eq. (1) such that

$$u_{1x}(x,y) = mu_{1x_1}^{(1)}(x_1,y_1)-nu_{1y_1}^{(1)}(x_1,y_1)+u_{1x}^{(2)}(x,y), \tag{42a}$$

$$u_{1y}(x,y) = nu_{1x_1}^{(1)}(x_1,y_1)+mu_{1y_1}^{(1)}(x_1,y_1)+u_{1y}^{(2)}(x,y), \tag{42b}$$

$$\sigma_{1xx}(x,y) = m^2\sigma_{1x_1x_1}^{(1)}(x_1,y_1)-2mn\sigma_{1x_1y_1}^{(1)}(x_1,y_1) + n^2\sigma_{1y_1y_1}^{(1)}(x_1,y_1)+\sigma_{1xx}^{(2)}(x,y), \tag{42c}$$

$$\sigma_{1xy}(x,y) = mn\left[\sigma_{1x_1x_1}^{(1)}(x_1,y_1)-\sigma_{1y_1y_1}^{(1)}(x_1,y_1)\right] + (m^2-n^2)\sigma_{1x_1y_1}^{(1)}(x_1,y_1)+\sigma_{1xy}^{(2)}(x,y). \tag{42d}$$

The state vectors, $\mathbf{f}_j(x,s)$, $j = 1, 2, 3$, containing the displacements and tractions in the bonded system are then defined in the Fourier-transformed domain (x,s) in the form as:

$$\mathbf{f}_j(x,s) = \left\{\bar{u}_{jx}(x,s)/i, \bar{u}_{jy}(x,s), \bar{\sigma}_{jxx}(x,s)/i, \bar{\sigma}_{jxy}(x,s)\right\}^T; \quad j = 1,2,3 \tag{43}$$

and from Eqs. (32), (34), (35), (41) and the constitutive relations in Eqs. (6a)–(6c), the vectors, $\mathbf{f}_j^{\pm}(s), j = 1,2,3$, evaluated at the right-(+) and left-hand side (−) surfaces of the constituents can be written as:

$$\mathbf{f}_1^-(s) = \mathbf{T}_1^-(s)\mathbf{a}_1+\mathbf{f}_{1T}^-(s)+\boldsymbol{\Psi}(s), \tag{44a}$$

$$\mathbf{f}_2^{\pm}(s) = \mathbf{T}_2^{\pm}(s)\mathbf{a}_2+\mathbf{f}_{2T}^{\pm}(s), \tag{44b}$$

$$\mathbf{f}_3^+(s) = \mathbf{T}_3^+(s)\mathbf{a}_3+\mathbf{f}_{3T}^+(s), \tag{44c}$$

where $\mathbf{T}_j^{\pm}(s), j = 1,2,3$, are matrices which are a function of not only the variable s, but also the elastic parameters of the constituents, and 4×4 for the interlayer ($j = 2$) and 4×2 for the half-planes ($j = 1,3$), while $\mathbf{a}_j(s)$, $j = 1, 2, 3$, are vectors for the unknowns in the general solutions of thermoelasticity equations such that

$$\mathbf{a}_1 = \{F_1(s),F_2(s)\}^T, \quad \mathbf{a}_2 = \{G_1(s),G_2(s),G_3(s),G_4(s)\}^T, \tag{45a,b}$$

$$\mathbf{a}_3 = \{H_1(s),H_2(s)\}^T \tag{45c}$$

and $\mathbf{f}_{jT}^{\pm}(s), j = 1,2,3$, are vectors that signify the nonisothermal effect originating from the nonhomogeneous part of the governing equations in Eqs. (8a) and (8b). In addition, $\boldsymbol{\Psi}(s)$ is a vector of four units in length whose elements are obtained by taking the Fourier transform of the full-plane solutions in Eq. (32) with respect to y-axis (see Appendix B).

By using the state vector equations, the interfacial conditions in Eqs. (27a)–(27d) can be expressed as:

$$\mathbf{T}_1^-(s)\mathbf{a}_1+\mathbf{f}_{1T}^-(s)+\boldsymbol{\Psi}(s) = \mathbf{T}_2^+(s)\mathbf{a}_2+\mathbf{f}_{2T}^+(s), \tag{46a}$$

$$\mathbf{T}_2^-(s)\mathbf{a}_2+\mathbf{f}_{2T}^-(s) = \mathbf{T}_3^+(s)\mathbf{a}_3+\mathbf{f}_{3T}^+(s) \tag{46b}$$

and the elimination of the unknown vector $\mathbf{a}_2(s)$ yields the following:

$$\mathbf{G}(s)\mathbf{a}_3+\mathbf{r}(s) = \mathbf{H}_1(s)\mathbf{a}_1+\boldsymbol{\Psi}(s), \tag{47}$$

where $\mathbf{G}(s)$ is a 4×2 transfer matrix between the two half-planes and $\mathbf{r}(s)$ is a vector of length four for the nonisothermal terms

$$\mathbf{G}(s) = \prod_{j=2}^{3}\mathbf{H}_j(s), \tag{48a}$$

$$\mathbf{r}(s) = \mathbf{H}_2(s)\left[\mathbf{f}_{3T}^+(s)-\mathbf{f}_{2T}^-(s)\right]+\mathbf{f}_{2T}^+(s)-\mathbf{f}_{1T}^-(s) \tag{48b}$$

in which the matrix functions, $\mathbf{H}_j(s)$, $j = 1, 2, 3$, are defined by:

$$\mathbf{H}_1(s) = \mathbf{T}_1^-(s), \quad \mathbf{H}_2(s) = \mathbf{T}_2^+(s)\left[\mathbf{T}_2^-(s)\right]^{-1}, \quad \mathbf{H}_3(s) = \mathbf{T}_3^+(s). \tag{49}$$

The transfer matrix equation in Eq. (47) can be decomposed and solved for the vectors, $\mathbf{a}_1(s)$ and $\mathbf{a}_3(s)$. In particular, the vector $\mathbf{a}_1(s)$ that is essentially required in deriving the integral equations for thermal stresses can be obtained in terms of the elements of the vectors, $\boldsymbol{\Psi}(s)$ and $\mathbf{r}(s)$, such that

$$\begin{Bmatrix}F_1\\F_2\end{Bmatrix} = \begin{bmatrix}Q_{11} & Q_{12}\\Q_{21} & Q_{22}\end{bmatrix}\begin{Bmatrix}f_{01}\\f_{02}\end{Bmatrix}, \tag{50}$$

where $Q_{ij}(s)$, $i,j = 1, 2$, are elements of a 2×2 matrix and $f_{0j}(s)$, $j = 1, 2$, are those of a vector of length two as

$$\mathbf{Q}(s)=\begin{bmatrix}H_{11}-M_{11} & H_{12}-M_{12}\\ H_{21}-M_{21} & H_{22}-M_{22}\end{bmatrix}^{-1} \tag{51a}$$

$$\mathbf{f}_0(s)=\begin{bmatrix}L_{11} & L_{12}\\ L_{21} & L_{22}\end{bmatrix}\begin{Bmatrix}\Psi_3-r_3\\ \Psi_4-r_4\end{Bmatrix}-\begin{Bmatrix}\Psi_1-r_1\\ \Psi_2-r_2\end{Bmatrix} \tag{51b}$$

in which $H_{ij}(s)$, $i=1,\ldots,4$, $j=1,2$, are elements of the matrix $\mathbf{H}_1(s)$, and $M_{ij}(s)$, $i,j=1,2$, and $L_{ij}(s)$, $i,j=1,2$, are those of 2×2 matrices

$$\mathbf{M}(s)=\begin{bmatrix}G_{11} & G_{12}\\ G_{21} & G_{22}\end{bmatrix}\begin{bmatrix}G_{31} & G_{32}\\ G_{41} & G_{42}\end{bmatrix}^{-1}\begin{bmatrix}H_{31} & H_{32}\\ H_{41} & H_{42}\end{bmatrix}, \tag{52a}$$

$$\mathbf{L}(s)=\begin{bmatrix}G_{11} & G_{12}\\ G_{21} & G_{22}\end{bmatrix}\begin{bmatrix}G_{31} & G_{32}\\ G_{41} & G_{42}\end{bmatrix}^{-1}. \tag{52b}$$

It is noted that the matrix $\mathbf{Q}(s)$ depends only on the elastic constants of the bonded system, and the vector $\mathbf{f}_0(s)$ has the dependency on the thermoelastic moduli and involves the functions ϕ_0 and ϕ_j, $j=1,2$.

4.2. Integral equations for thermal stresses

The remaining traction-free crack surface conditions in the (x_1,y_1) coordinates are written from Eqs. (28c) and (30b) as:

$$\begin{aligned}&\sigma_{1y_1y_1}(x_1,+0)=\sigma^{(1)}_{1y_1y_1}(x_1,+0)+\sigma^{(2)}_{1y_1y_1}(x_1,+0)=0;\quad a<x_1<b,\\ &\sigma_{1x_1y_1}(x_1,+0)=\sigma^{(1)}_{1x_1y_1}(x_1,+0)\\ &\quad+\sigma^{(2)}_{1x_1y_1}(x_1,+0)=0;\quad a<x_1<b,\end{aligned} \tag{53a,b}$$

where the first terms on the right-hand side are evaluated from Eqs. (32d) and (32e) as the integrals with Cauchy singular kernels

$$\frac{\pi(1+\kappa)}{2\mu_1}\lim_{y_1\to+0}\sigma^{(1)}_{1y_1y_1}(x_1,y_1)=\int_a^b\frac{\phi_1(t)}{t-x_1}dt, \tag{54a}$$

$$\begin{aligned}\frac{\pi(1+\kappa)}{2\mu_1}\lim_{y_1\to+0}\sigma^{(1)}_{1x_1y_1}(x_1,y_1)&=\int_a^b\frac{\phi_2(t)}{t-x_1}dt\\ &\quad+\alpha_1^*\int_a^b\phi_0(t)\ln|t-x_1|dt\end{aligned} \tag{54b}$$

and the second terms transformed from the (x,y) coordinates to the (x_1,y_1) coordinates are expressed as:

$$\sigma^{(2)}_{1y_1y_1}(x_1,y_1)=n^2\sigma^{(2)}_{1xx}(x,y)-2mn\sigma^{(2)}_{1xy}(x,y)+m^2\sigma^{(2)}_{1yy}(x,y), \tag{55a}$$

$$\sigma^{(2)}_{1x_1y_1}(x_1,y_1)=mn\left[\sigma^{(2)}_{1yy}(x,y)-\sigma^{(2)}_{1xx}(x,y)\right]+(m^2-n^2)\sigma^{(2)}_{1xy}(x,y), \tag{55b}$$

so that from Eqs. (6), (34), and (22b), it can be shown that

$$\begin{aligned}&\frac{\pi}{\mu_1}\lim_{y_1\to+0}\sigma^{(2)}_{1y_1y_1}(x_1,y_1)\\ &\quad=\int_{-\infty}^{\infty}\{F_1[N_{11}(s,x_1)+iN_{12}(s,x_1)]\\ &\quad+F_2[N_{13}(s,x_1)+iN_{14}(s,x_1)]\}e^{-(m|s|+ins)x_1}ds\\ &\quad+\frac{2\alpha_1^*}{1+\kappa}\int_{-\infty}^{\infty}A[X_{11}(s,x_1)+iX_{12}(s,x_1)]e^{-(m|s|+ins)x_1}ds\end{aligned} \tag{56a}$$

$$\begin{aligned}&\frac{\pi}{\mu_1}\lim_{y_1\to+0}\sigma^{(2)}_{1x_1y_1}(x_1,y_1)\\ &\quad=\int_{-\infty}^{\infty}\{F_1[N_{21}(s,x_1)+iN_{22}(s,x_1)]\\ &\quad+F_2[N_{23}(s,x_1)+iN_{24}(s,x_1)]\}e^{-(m|s|+ins)x_1}ds\\ &\quad+\frac{2\alpha_1^*}{1+\kappa}\int_{-\infty}^{\infty}A[X_{21}(s,x_1)+iX_{22}(s,x_1)]e^{-(m|s|+ins)x_1}ds\end{aligned} \tag{56b}$$

in which $N_{ij}(s,x_1)$, $i=1,2$, $j=1,\ldots,4$, and $X_{ij}(s,x_1)$, $i,j=1,2$, are given by:

$$N_{11}(s,x_1)=2mn|s|,\quad N_{12}(s,x_1)=(n^2-m^2)s, \tag{57a}$$

$$\begin{aligned}N_{13}(s,x_1)&=mn(2m|s|x_1-1+\kappa),\\ N_{14}(s,x_1)&=(n^2-m^2)\left(msx_1-\frac{|s|}{s}\frac{1-\kappa}{2}\right)+\frac{|s|}{s},\end{aligned} \tag{57b}$$

$$N_{21}(s,x_1)=(n^2-m^2)|s|,\quad N_{22}(s,x_1)=-2mns, \tag{57c}$$

$$\begin{aligned}N_{23}(s,x_1)&=(n^2-m^2)\left(m|s|x_1-\frac{1-\kappa}{2}\right),\\ N_{24}(s,x_1)&=mn\left[\frac{|s|}{s}(1-\kappa)-2msx_1\right],\end{aligned} \tag{57d}$$

$$\begin{aligned}X_{11}(s,x_1)&=-m(n^2-m^2)|s|x_1-2m^2,\\ X_{12}(s,x_1)&=2mn\left(msx_1-\frac{|s|}{s}\right),\end{aligned} \tag{57e}$$

$$\begin{aligned}X_{21}(s,x_1)&=-2mn(1-m|s|x_1),\\ X_{22}(s,x_1)&=(n^2-m^2)\left(msx_1-\frac{|s|}{s}\right).\end{aligned} \tag{57f}$$

Upon substituting Eqs. (54) and (56) into Eq. (53) and using the expressions of $F_j(s)$, $j=1,2$, in Eq. (50) and $A(s)$ in Eq. (A.1), followed by some algebraic manipulations, a system of Cauchy-type singular integral equations is derived for the thermal stress analysis in the form as:

$$\begin{aligned}&\int_a^b\frac{\phi_1(t)}{t-x_1}dt+\int_a^b\sum_{j=1}^{2}k_{1j}(x_1,t)\phi_j(t)dt\\ &\quad=\int_a^b\left[\alpha_1^*g_{12}(x_1,t)-g_{11}(x_1,t)\right]\phi_0(t)dt;\quad a<x_1<b,\end{aligned} \tag{58a}$$

$$\begin{aligned}&\int_a^b\frac{\phi_2(t)}{t-x_1}dt+\int_a^b\sum_{j=1}^{2}k_{2j}(x_1,t)\phi_j(t)dt\\ &\quad=\int_a^b\left[\alpha_1^*g_{22}(x_1,t)-g_{21}(x_1,t)-\alpha_1^*\ln|t-x_1|\right]\phi_0(t)dt;\quad a<x_1<b,\end{aligned} \tag{58b}$$

where the kernels $k_{ij}(x_1,t)$, $i,j=1,2$, and $g_{ij}(x_1,t)$, $i,j=1,2$, are written as:

$$\begin{aligned}&k_{ij}(x_1,t)\\ &\quad=\int_0^{\infty}\left[\Lambda_{ij}(s,x_1,t)\cos ns(t-x_1)\right.\\ &\quad\left.-\Lambda_{i(j+2)}(s,x_1,t)\sin ns(t-x_1)\right]e^{-ms(t+x_1)}ds;\quad i,j=1,2,\end{aligned} \tag{59a}$$

$$\begin{aligned}&g_{ij}(x_1,t)\\ &=\int_0^{\infty}\left[\Gamma_{ij}(s,x_1,t)\cos ns(t-x_1)\right.\\ &\left.-\Gamma_{i(j+1)}(s,x_1,t)\sin ns(t-x_1)\right]e^{-ms(t+x_1)}ds;\ (i,j)=(1,1),(2,1),\end{aligned} \tag{59b}$$

$$\begin{aligned}&g_{ij}(x_1,t)\\ &\quad=\int_0^{\infty}\frac{1}{s}\Lambda_0(s)\left[X_{i(j-1)}(s,x_1)\sin ns(t-x_1)\right.\\ &\quad\left.+X_{ij}(s,x_1)\cos ns(t-x_1)\right]e^{-ms(t+x_1)}ds;\quad (i,j)=(1,2),(2,2)\end{aligned} \tag{59c}$$

in which $\Lambda_{ij}(s,x_1,t)$, $i=1,2$, $j=1,\ldots,4$, and $\Gamma_{ij}(s,x_1,t)$, $i,j=1,2$, are intricate functions of isothermal and nonisothermal moduli, respectively, as well as the geometry of the bonded trimaterial system.

The integrands of the kernels in Eqs. (59a)–(59c) retain the exponentially decaying behavior as the variable s tends to be large, indicating that the kernels are bounded. On the other hand, the disappearance of the exponential decay that is noted when $\theta \to 90°$ or $(t + x_1) \to 0.0$ renders the convergence rate of related improper integrals relatively slower than they would be otherwise. The former is for a crack lying along or parallel to the nominal interface and the latter is associated with a crack that has its tip extended up to the interface. In particular, when $d = 0.0$ and $0° \leqslant \theta \leqslant 90°$, it can be shown that there exist logarithmic terms in the kernels other than $\ln|t - x_1|$ in Eq. (58b), as discussed by Erdogan (1998) for the two special cases of $\theta = 0°$ and $\theta = 90°$. Such logarithmic terms, nonetheless, can be treated as part of regular kernels in the presence of Cauchy singular kernels $1/(t - x_1)$ in the sense that the logarithmic singularities are square-integrable, without affecting the near-tip singular order of the thermoelastic field in the oblique crack configuration, provided the thermoelastic moduli are continuous and piecewise differentiable near and at the crack tip. This is in contrast to the oscillatory or nonsquare-root singularities encountered in the analysis of crack problems for bonded media which are of piecewise homogeneous nature (Rice, 1988; Romeo and Ballarini, 1995).

5. Solution procedure and near-tip field intensity factors

Because the dominant singular kernels in the integral equations are attributable solely to the Cauchy type, the square-root crack-tip behavior of the problem can be preserved by expressing the auxiliary functions as (Muskhelishvili, 1953)

$$\phi_j(t) = \frac{\varphi_j(t)}{\sqrt{(t-a)(b-t)}}; \quad a < t < b,\ j = 0, 1, 2, \tag{60}$$

where $\varphi_j(t)$, $j = 0, 1, 2$, are unknown functions, bounded and nonzero at the end points. In the normalized interval

$$\begin{Bmatrix} t \\ x_1 \end{Bmatrix} = \frac{b-a}{2}\begin{Bmatrix} \eta \\ \xi \end{Bmatrix} + \frac{b+a}{2}; \quad -1 < (\eta, \xi) < 1, \tag{61}$$

the integral equations in Eqs. (24) and (58) are rewritten as:

$$\int_{-1}^{1} \frac{\phi_0(\eta)}{\eta - \xi} d\eta + \frac{b-a}{2}\int_{-1}^{1} k_0(\xi, \eta)\phi_0(\eta) d\eta - 2\pi\lambda_b \int_{-1}^{\xi} \phi_0(\eta) d\eta = -2\pi \nabla T_\infty; \quad |\xi| < 1, \tag{62a}$$

$$\int_{-1}^{1} \frac{\phi_1(\eta)}{\eta - \xi} d\eta + \frac{b-a}{2}\int_{-1}^{1} \sum_{j=1}^{2} k_{1j}(\xi, \eta)\phi_j(\eta) d\eta = \frac{b-a}{2}\int_{-1}^{1} h_1(\xi, \eta)\phi_0(\eta) d\eta; \quad |\xi| < 1, \tag{62b}$$

$$\int_{-1}^{1} \frac{\phi_2(\eta)}{\eta - \xi} d\eta + \frac{b-a}{2}\int_{-1}^{1} \sum_{j=1}^{2} k_{2j}(\xi, \eta)\phi_j(\eta) d\eta = \frac{b-a}{2}\int_{-1}^{1} [h_2(\xi, \eta) - \alpha_1^* \ln|\eta - \xi|]\phi_0(\eta) d\eta; \quad |\xi| < 1 \tag{62c}$$

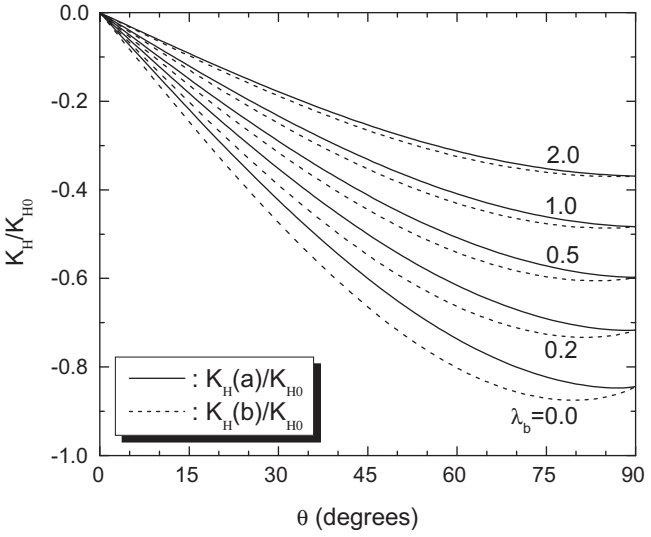

Fig. 3. Variations of heat-flux intensity factors K_H/K_{H0} as a function of θ under a horizontal heat flow $\left(\nabla T_x^\infty = \nabla T, \nabla T_y^\infty = 0\right)$ for different values of λ_b where $K_{H0} = k_1 \nabla T c^{1/2}$, $h/2c = 0.5$, and $d/c = 0.0$.

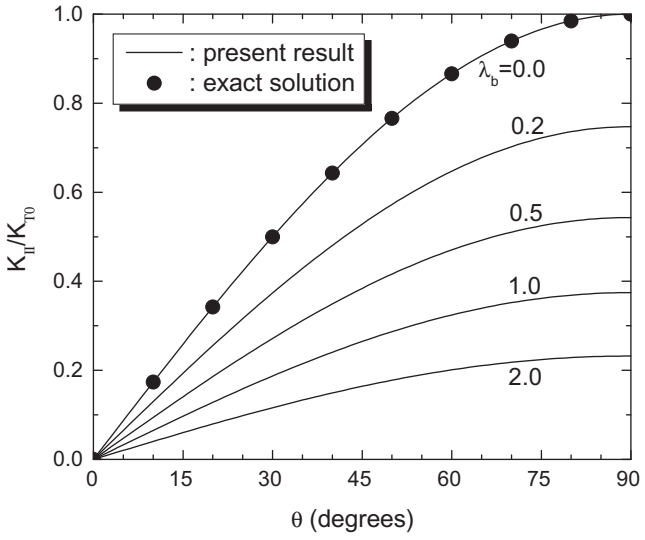

Fig. 2. Variations of mode II thermal-stress intensity factors K_{II}/K_{T0} as a function of θ in an infinite homogeneous plane under a horizontal heat flow $(\nabla T_x^\infty = \nabla T, \nabla T_y^\infty = 0)$ for different values of λ_b where $K_{T0} = 2\mu\alpha^* \nabla T c^{3/2}/(1 + \kappa)$.

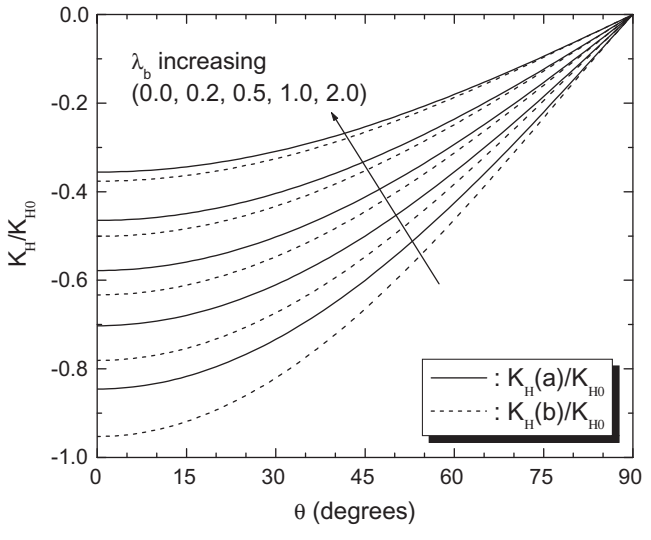

Fig. 4. Variations of heat-flux intensity factors K_H/K_{H0} as a function of θ under a vertical heat flow $\left(\nabla T_y^\infty = \nabla T, \nabla T_x^\infty = 0\right)$ for different values of λ_b where $K_{H0} = k_1 \nabla T\, c^{1/2}$, $h/2c = 0.5$, and $d/c = 0.0$.

in which $h_j(\xi,\eta)=\alpha_1^* g_{j2}(\xi,\eta)-g_{j1}(\xi,\eta), j=1,2$, and $\lambda_b = h_c c/k_1$ in Eq. (62a) is the *Biot number*, as the dimensionless ratio between heat conductance at the crack surfaces and the conductivity of the cracked constituent, to describe the degree of crack-surface partial insulation (Barber, 1980). As is evident in the foregoing, the integral equation in Eq. (62a) for heat conduction should first be independently solved for ϕ_0, with the corresponding results made available for incorporation as the forcing terms in solving the system of integral equations in Eqs. (62b) and (62c) for thermal stress analysis.

The solutions to the singular integral equations can, therefore, be expanded into the series of the Chebyshev polynomials of the first kind T_n as:

$$\phi_j(t)=\phi_j(\eta)=\frac{1}{\sqrt{1-\eta^2}}\sum_{n=0}^{\infty}c_{jn}T_n(\eta);\quad |\eta|<1,\ j=0,1,2 \tag{63}$$

where c_{jn}, $j=0,\ 1,\ 2$, $n\geqslant 0$, are unknown coefficients and via the orthogonality for T_n, the compatibility conditions in Eqs. (15b) and (33b) are identically satisfied when $c_{j0}=0$, $j=0,\ 1,\ 2$.

After substituting Eq. (63) into Eqs. (62a)–(62c), truncating the series with the first N terms, and using the properties of the Chebyshev polynomials (Gradshteyn and Ryzhik, 2000), one can show that the integral equations are regularized

$$\sum_{n=1}^{N}c_{0n}\left[\pi\left(1+\frac{2\lambda_b}{n}\sqrt{1-\xi^2}\right)U_{n-1}(\xi)+H_0^n(\xi)\right]=-2\pi\nabla T_\infty;\quad |\xi|<1,$$

$$\pi\sum_{n=1}^{N}\begin{Bmatrix}c_{1n}\\ c_{2n}\end{Bmatrix}U_{n-1}(\xi)+\sum_{n=1}^{N}\begin{bmatrix}H_{11}^n(\xi) & H_{12}^n(\xi)\\ H_{21}^n(\xi) & H_{22}^n(\xi)\end{bmatrix}\begin{Bmatrix}c_{1n}\\ c_{2n}\end{Bmatrix}=\begin{Bmatrix}f_1(\xi)\\ f_2(\xi)\end{Bmatrix};\quad |\xi|<1 \tag{64a,b}$$

where U_n are the Chebyshev polynomials of the second kind and the functions, $H_0^n(\xi)$ and $H_{ij}^n(\xi), i,j=1,2$, are given by

$$H_0^n(\xi)=\frac{b-a}{2}\int_{-1}^{1}\frac{k_0(\xi,\eta)T_n(\eta)}{\sqrt{1-\eta^2}}d\eta, \tag{65a}$$

$$H_{ij}^n(\xi)=\frac{b-a}{2}\int_{-1}^{1}\frac{k_{ij}(\xi,\eta)T_n(\eta)}{\sqrt{1-\eta^2}}d\eta;\quad i,j=1,2 \tag{65b}$$

while the forcing functions, $f_j(\xi)$, $j=1,\ 2$, that contain the thermal loading are defined as:

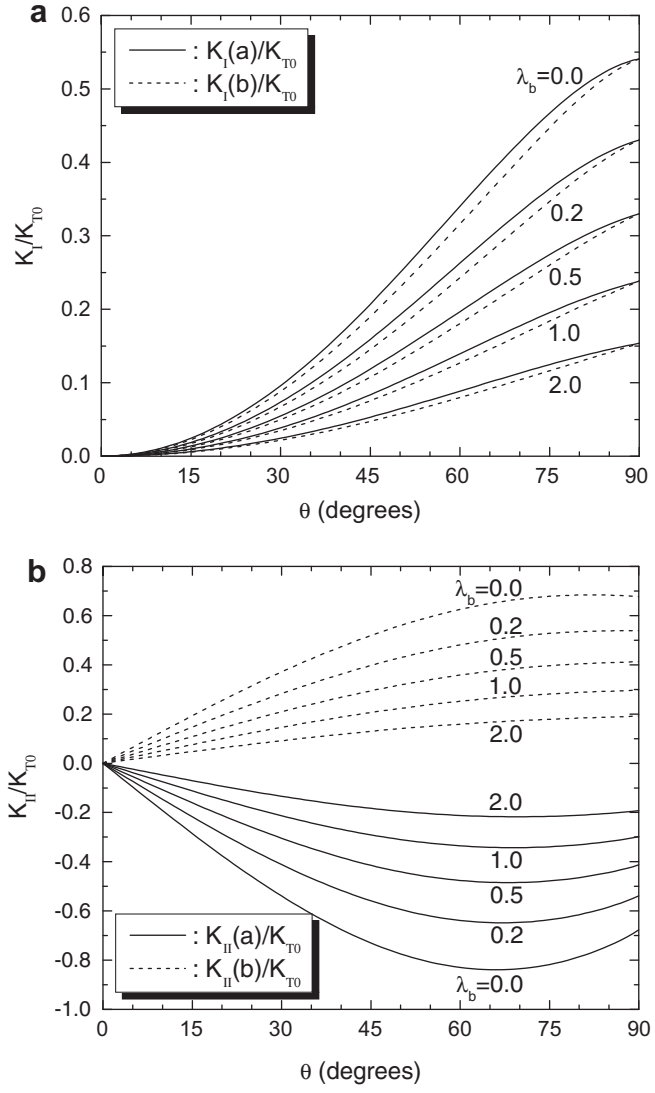

Fig. 5. Variations of thermal-stress intensity factors (a) K_I/K_{T0} and (b) K_{II}/K_{T0} as a function of θ under a horizontal heat flow $\left(\nabla T_x^\infty=\nabla T, \nabla T_y^\infty=0\right)$ for different values of λ_b where $K_{T0}=2\mu_1\alpha_1^*\nabla T c^{3/2}/(1+\kappa), h/2c=0.5$, and $d/c=0.0$.

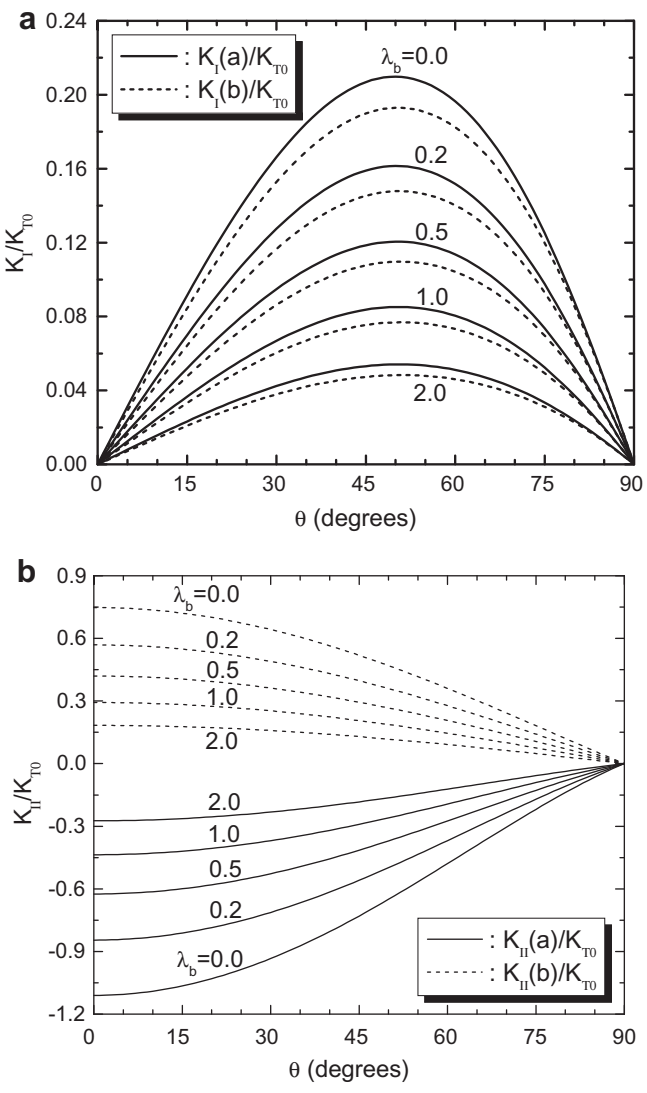

Fig. 6. Variations of thermal-stress intensity factors (a) K_I/K_{T0} and (b) K_{II}/K_{T0} as a function of θ under a vertical heat flow $\left(\nabla T_y^\infty=\nabla T, \nabla T_x^\infty=0\right)$ for different values of λ_b where $K_{T0}=2\mu_1\alpha_1^*\nabla T c^{3/2}/(1+\kappa), h/2c=0.5$, and $d/c=0.0$.

$$f_1(\xi) = \frac{b-a}{2}\sum_{n=1}^{N} c_{0n}\int_{-1}^{1}\frac{h_1(\xi,\eta)T_n(\eta)}{\sqrt{1-\eta^2}}d\eta, \tag{66a}$$

$$f_2(\xi) = \frac{b-a}{2}\sum_{n=1}^{N} c_{0n}\left[\int_{-1}^{1}\frac{h_2(\xi,\eta)T_n(\eta)}{\sqrt{1-\eta^2}}d\eta + \frac{\alpha_1^*\pi}{n}T_n(\xi)\right]. \tag{66b}$$

To recast the functional equations in Eqs. (64a) and (64b) into solvable form, the zeros of T_N concentrated near the ends $\xi = \pm 1$ are chosen as a set of collocation points (Erdogan, 1978)

$$T_N(\xi_j) = 0, \xi_j = \cos\left[\frac{\pi(2j-1)}{2N}\right]; \quad j = 1, 2, \ldots, N \tag{67}$$

and by evaluating Eq. (64a) at N station points ξ_j, a system of linear algebraic equations is constructed and solved for c_{0n}, $1 \leqslant n \leqslant N$, to be incorporated into Eqs. (66a) and (66b). Likewise, the equations in Eq. (64b) can then be reduced to a system of linear algebraic equations for c_{jn}, $j = 1, 2$, $1 \leqslant n \leqslant N$.

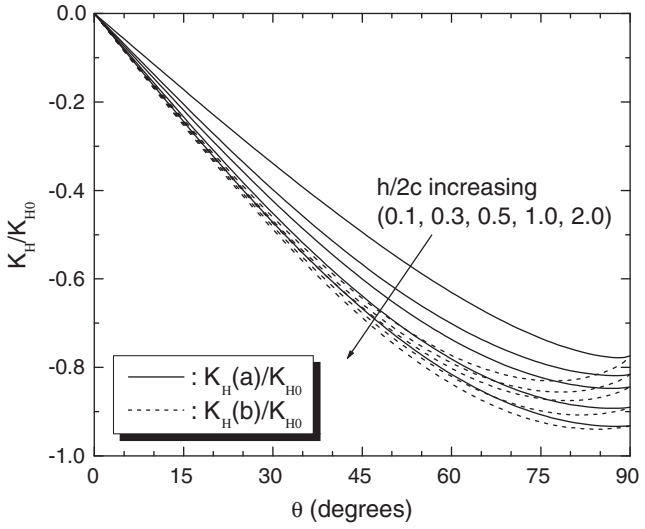

Fig. 7. Variations of heat-flux intensity factors K_H/K_{H0} as a function of θ under a horizontal heat flow $\left(\nabla T_x^\infty = \nabla T, \nabla T_y^\infty = 0\right)$ for different values of $h/2c$ where $K_{H0} = k_1\nabla T c^{1/2}$, $\lambda_b = 0.0$, and $d/c = 0.0$.

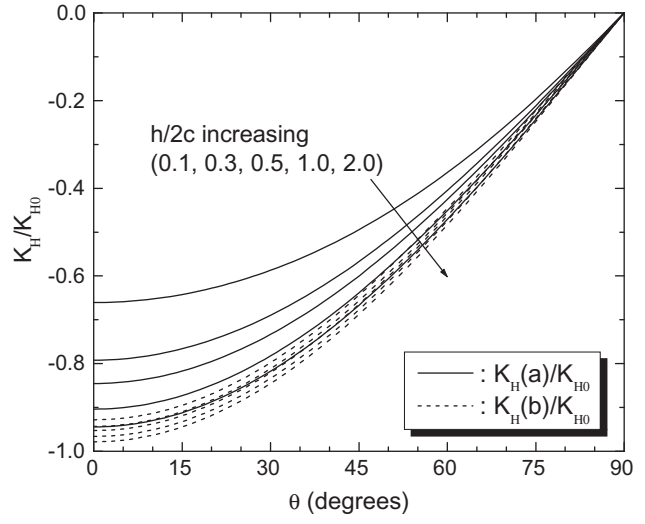

Fig. 8. Variations of heat-flux intensity factors K_H/K_{H0} as a function of θ under a vertical heat flow $\left(\nabla T_y^\infty = \nabla T, \nabla T_x^\infty = 0\right)$ for different values of $h/2c$ where $K_{H0} = k_1\nabla T c^{1/2}$, $\lambda_b = 0.0$, and $d/c = 0.0$.

Once the coefficients, c_{jn}, $j = 0, 1, 2$, $1 \leqslant n \leqslant N$, are obtained, the integral equations in Eq. (24) and Eq. (58) can provide the values of heat flux, $q_{1y_1}(x_1, 0)$, and tractions, $\sigma_{1y_1y_1}(x_1, 0)$ and $\sigma_{1x_1y_1}(x_1, 0)$, ahead of crack tips, respectively, that both possess the inverse square-root singular behavior. The singular thermal behavior implies the thermal energy localization in heat conduction around the crack and such intensified energy would exert an adverse effect in dissipating the heat. In order to measure the magnitude of local intensification of the thermal field at the point of singularity and to signify the thermal energy accumulated in the near-tip region as well, the heat-flux intensity factors K_H can be defined and evaluated as (Tzou, 1991)

$$K_H(a) = \lim_{x_1\to a}\sqrt{2(a-x_1)}q_{1y_1}(x_1,0) = \frac{k_1}{2}\sqrt{\frac{b-a}{2}}\sum_{n=1}^{N}(-1)^{n+1}c_{0n}; \quad x_1 < a, \tag{68a}$$

$$K_H(b) = \lim_{x_1\to b}\sqrt{2(x_1-b)}q_{1y_1}(x_1,0) = \frac{k_1}{2}\sqrt{\frac{b-a}{2}}\sum_{n=1}^{N}c_{0n}; \quad x_1 > b. \tag{68b}$$

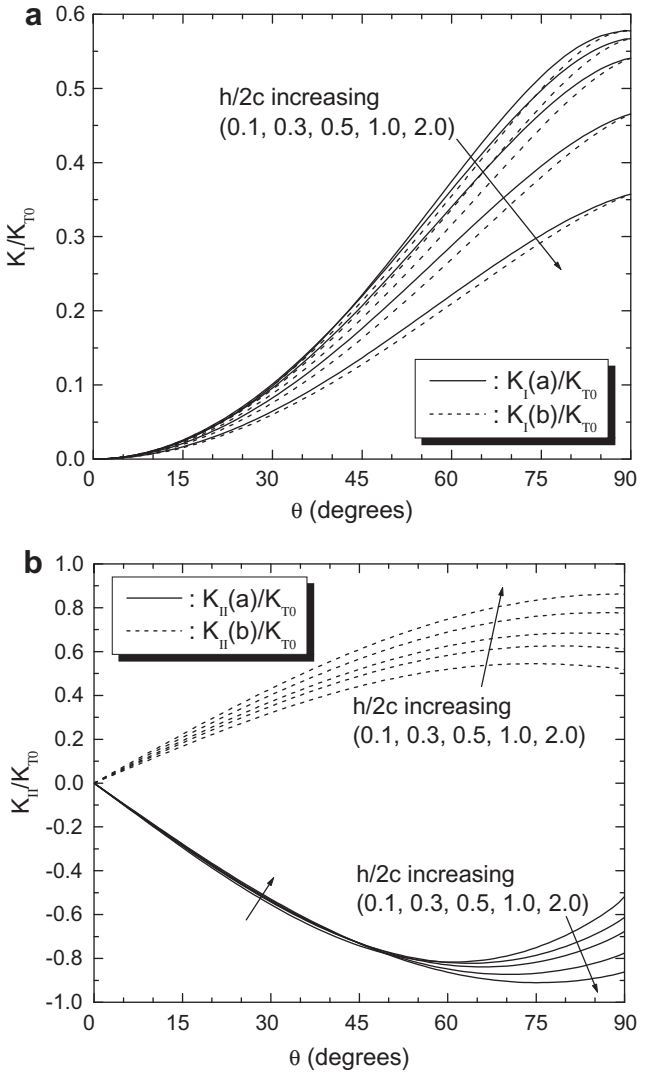

Fig. 9. Variations of thermal-stress intensity factors (a) K_I/K_{T0} and (b) K_{II}/K_{T0} as a function of θ under a horizontal heat flow $\left(\nabla T_x^\infty = \nabla T, \nabla T_y^\infty = 0\right)$ for different values of $h/2c$ where $K_{T0} = 2\mu_1\alpha_1^*\nabla T c^{3/2}/(1+\kappa)$, $\lambda_b = 0.0$, and $d/c = 0.0$.

Furthermore, to characterize the severity of near-tip thermal stresses that develop in turn, the mixed-mode stress intensity factors are also defined and evaluated such that

$$\begin{Bmatrix} K_{\mathrm{I}}(a) \\ K_{\mathrm{II}}(a) \end{Bmatrix} = \lim_{x_1 \to a} \sqrt{2(a-x_1)} \begin{Bmatrix} \sigma_{1y_1y_1}(x_1,0) \\ \sigma_{1x_1y_1}(x_1,0) \end{Bmatrix} = \frac{2\mu_1}{1+\kappa}\sqrt{\frac{b-a}{2}}\sum_{n=1}^{N}(-1)^n \begin{Bmatrix} c_{1n} \\ c_{2n} \end{Bmatrix}; \quad x_1 < a, \tag{69a}$$

$$\begin{Bmatrix} K_{\mathrm{I}}(b) \\ K_{\mathrm{II}}(b) \end{Bmatrix} = \lim_{x_1 \to b} \sqrt{2(x_1-b)} \begin{Bmatrix} \sigma_{1y_1y_1}(x_1,0) \\ \sigma_{1x_1y_1}(x_1,0) \end{Bmatrix} = -\frac{2\mu_1}{1+\kappa}\sqrt{\frac{b-a}{2}}\sum_{n=1}^{N} \begin{Bmatrix} c_{1n} \\ c_{2n} \end{Bmatrix}; \quad x_1 > b, \tag{69b}$$

where K_{I} and K_{II} are modes I and II stress intensity factors, respectively, and due to the continuity of thermoelastic moduli through the graded interlayer, the field intensity factors in the preceding equations are equally valid for $d = 0.0$ as well, in which one of the crack tip is terminated at the location of nominal interface with the interlayer.

6. Results and discussion

The integral equations in Eqs. (24) and Eq. (58) are solved for various combinations of geometric $(\theta, h/2c, d/c)$ and thermoelastic parameters $(\lambda_b, k_3/k_1, \mu_3/\mu_1, \alpha_3/\alpha_1)$ of the problem under consideration. The state of plane strain is assumed with the constant Poisson's ratio $\nu = 0.3$. In the numerical implementation, no more than thirty-term expansions of the Chebyshev polynomials in Eq. (63) are found to be sufficient for the solution to converge with the desired level of accuracy, with the kernels in Eqs. (25a) and (59) and the other related integrals in Eqs. (65) and (66) being evaluated based on the Gauss–Legendre and Gauss–Chebyshev quadratures, respectively (Davis and Rabinowitz, 1984).

To confirm the validity of the current method of solutions, the problem of a homogeneous plane of infinite extent containing a partially insulated crack and subjected to a steady-state heat flow in the horizontal direction ($\nabla T_x^{\infty} = \nabla T$ and $\nabla T_y^{\infty} = 0$) is first

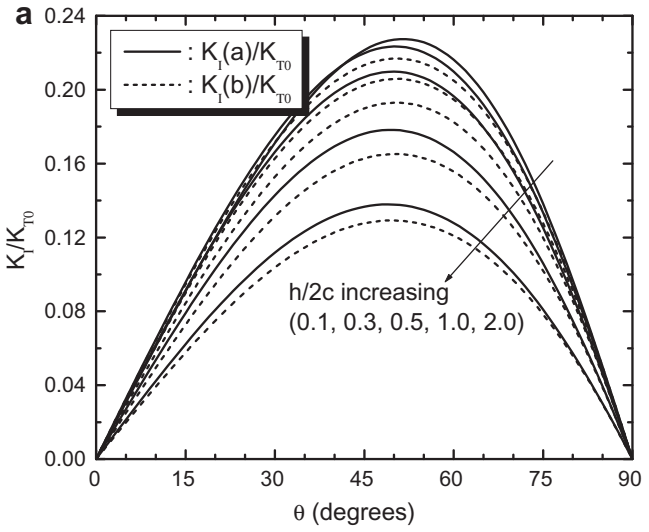

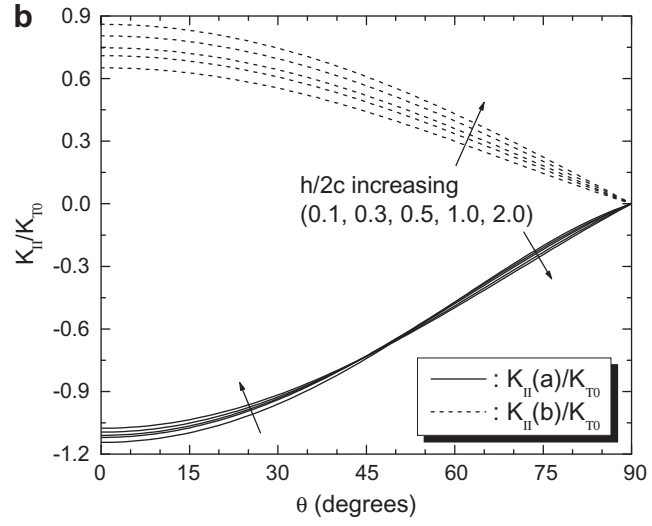

Fig. 10. Variations of thermal-stress intensity factors (a) K_{I}/K_{T0} and (b) K_{II}/K_{T0} as a function of θ under a vertical heat flow $\left(\nabla T_y^{\infty} = \nabla T, \nabla T_x^{\infty} = 0\right)$ for different values of $h/2c$ where $K_{T0} = 2\mu_1\alpha_1^*\nabla T c^{3/2}/(1+\kappa)$, $\lambda_b = 0.0$, and $d/c = 0.0$.

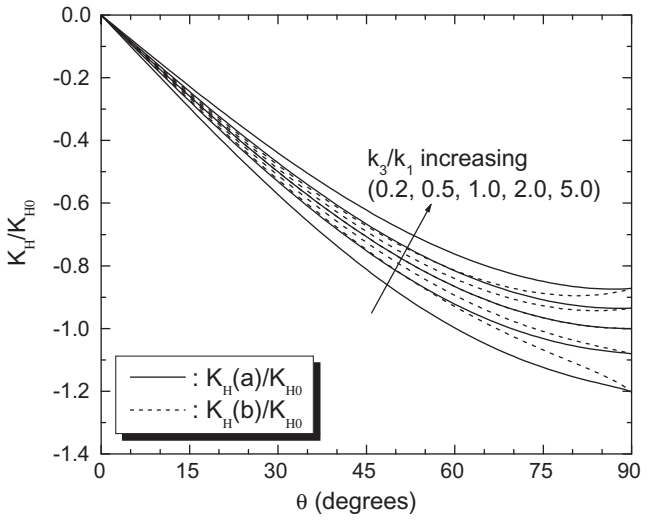

Fig. 11. Variations of heat-flux intensity factors $K_{\mathrm{H}}/K_{\mathrm{H0}}$ as a function of θ under a horizontal heat flow $\left(\nabla T_x^{\infty} = \nabla T, \nabla T_y^{\infty} = 0\right)$ for different values of k_3/k_1 where $K_{\mathrm{H0}} = k_1\nabla T c^{1/2}$, $\lambda_b = 0.0$, $h/2c = 0.5$, and $d/c = 0.0$.

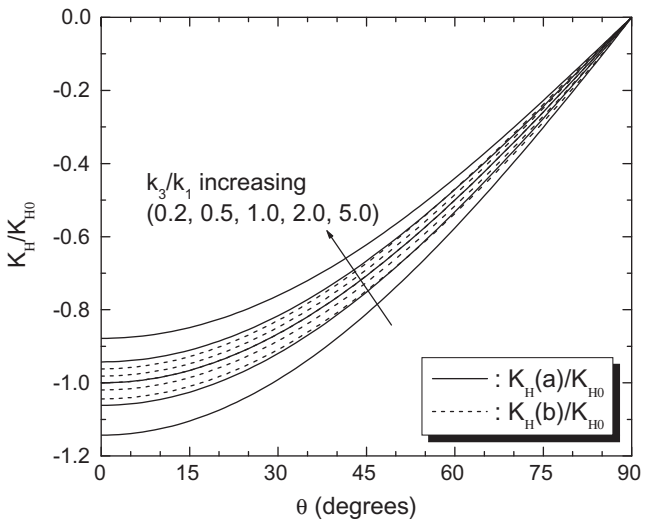

Fig. 12. Variations of heat-flux intensity factors $K_{\mathrm{H}}/K_{\mathrm{H0}}$ as a function of θ under a vertical heat flow $\left(\nabla T_y^{\infty} = \nabla T, \nabla T_x^{\infty} = 0\right)$ for different values of k_3/k_1 where $K_{\mathrm{H0}} = k_1\nabla T c^{1/2}$, $\lambda_b = 0.0$, $h/2c = 0.5$, and $d/c = 0.0$.

considered. In this case, the crack surfaces separate only in the sliding or shear mode, regardless of crack orientation angle θ. The variations of corresponding mode II thermal-stress intensity factors K_{II} are plotted in Fig. 2 as a function of θ, for different values of the Biot number λ_b. It is noted that the present values of K_{II} are those at the right-hand side crack tip and normalized with $K_{T0} = 2\mu\alpha^* \nabla T c^{3/2}/(1+\kappa)$, which is for a fully insulated crack ($\lambda_b = 0.0$) aligned perpendicular to the heat flow direction, and those evaluated for this insulated crack are in exact agreement with the closed form solution (Sekine, 1987). With the crack-surface thermal condition being relaxed via λ_b greater than zero, the severity of the thermal stress field around the crack is shown to be significantly alleviated, leading to nonconservative results in comparison with those obtained under the imposition of perfect crack-surface insulation.

As a next step toward predicting the thermally-induced crack-tip singularities in the bonded system, a metal/ceramic pair that is representative of titanium-based alloy (Ti-6Al-4V) bonded to zirconia (ZrO_2) is selected, with the ratios of thermoelastic moduli given by $k_3/k_1 = 8.89$, $\mu_3/\mu_1 = 0.5658$, $\alpha_3/\alpha_1 = 1.4487$ (Fujimoto and Noda, 2001) and $h/2c = 0.5$, $d/c = 0.0$, unless otherwise stated. Subsequently, further results are provided for the purpose of gaining an insight into the effects of variations of thermoelastic properties ($k_3/k_1, \mu_3/\mu_1, \alpha_3/\alpha_1$) on the crack-tip behavior in the prescribed thermal loading environment. In this process, the resulting values of the field intensity factors are discussed for each of the heat flows in the horizontal and vertical directions.

Under the condition that the crack surfaces are partially insulated in the above material pair, the variations of heat-flux intensity factors K_H versus the crack obliquity θ are illustrated Figs. 3 and 4, under a steady-state heat flow in the horizontal direction ($\nabla T_x^\infty = \nabla T$ and $\nabla T_y^\infty = 0$) and in the vertical direction ($\nabla T_y^\infty = \nabla T$ and $\nabla T_x^\infty = 0$), respectively. The results are normalized by $K_{H0} = k_1 \nabla T c^{1/2}$. A generic feature is that with no thermal disorder prevalent for the crack parallel to the direction of heat flow, the magnitude of K_H increases as the angle between the crack line and the heat flow direction is enlarged, but reduces as the crack surfaces are rendered heat conductive ($\lambda_b > 0.0$). Besides, it is understood that the more harsh thermal condition endured by the crack tip b is attributed to the mitigated effect of higher thermal conductivity of the adjacent constituent.

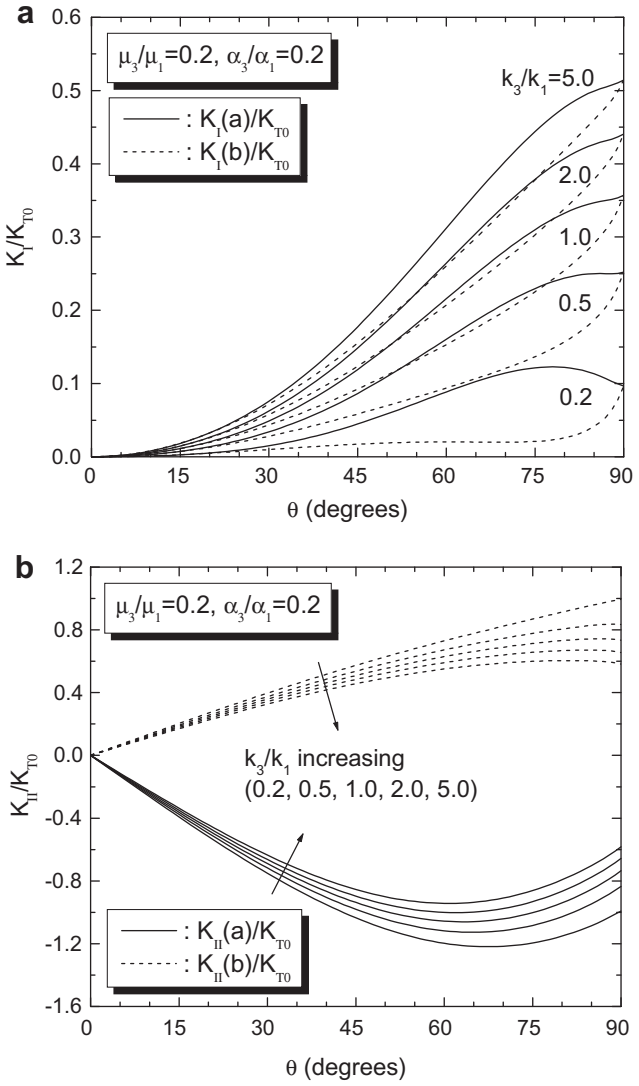

Fig. 13. Variations of thermal-stress intensity factors (a) K_I/K_{T0} and (b) K_{II}/K_{T0} as a function of θ under a horizontal heat flow $\left(\nabla T_x^\infty = \nabla T, \nabla T_y^\infty = 0\right)$ for different values of k_3/k_1 with $\mu_3/\mu_1 = 0.2$ and $\alpha_3/\alpha_1 = 0.2$ where $K_{T0} = 2\mu_1\alpha_1^*\nabla T c^{3/2}/(1+\kappa), \lambda_b = 0.0, h/2c = 0.5$, and $d/c = 0.0$.

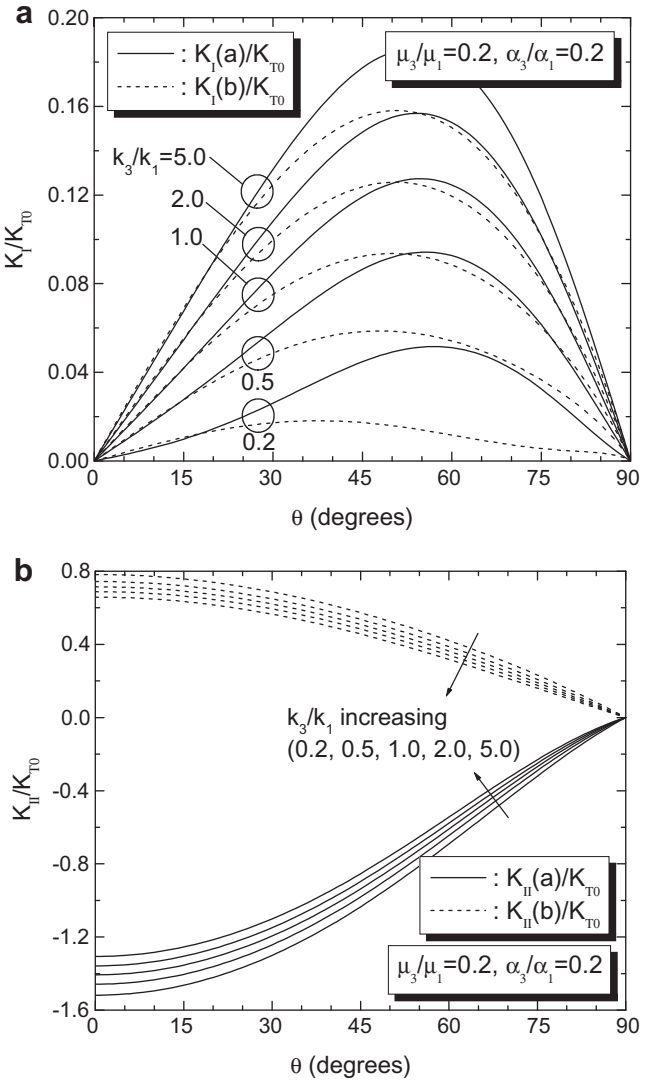

Fig. 14. Variations of thermal-stress intensity factors (a) K_I/K_{T0} and (b) K_{II}/K_{T0} as a function of θ under a vertical heat flow $\left(\nabla T_y^\infty = \nabla T, \nabla T_x^\infty = 0\right)$ for different values of k_3/k_1 with $\mu_3/\mu_1 = 0.2$ and $\alpha_3/\alpha_1 = 0.2$ where $K_{T0} = 2\mu_1\alpha_1^*\nabla T c^{3/2}/(1+\kappa), \lambda_b = 0.0, h/2c = 0.5$, and $d/c = 0.0$.

The variations of mixed-mode thermal-stress intensity factors that correspond to Figs. 3 and 4 are displayed in Figs. 5 and 6, respectively, with the normalizing quantity $K_{T0} = 2\mu_1\alpha_1^*\nabla Tc^{3/2}/(1+\kappa)$, where the severity of near-tip thermal stresses is also shown to be relieved as the crack becomes conductive with $\lambda_b > 0.0$. In contrast to the thermal behavior, however, the results in Figs. 5 and 6 indicate that the crack tip a is suffering from the rather intensified near-tip stress field such that both the values of thermal-stress intensity factors, K_I and K_{II}, at the crack tip a are of greater magnitude than those at the crack tip b. To be specific, as shown in Figs. 5a and 5b for the heat flowing in the horizontal direction, when the crack orientation angle θ is enlarged, the magnitudes of K_I and K_{II} are, in general, augmented in a monotonous manner from the null values at $\theta = 0°$ to their maxima that are matched with the interfacial cracking at $\theta = 90°$. It is worth mentioning for Fig. 6 that under the vertical heat flow that impinges on the crack surfaces perpendicularly as $\theta = 0°$, the antisymmetry of the temperature gradient, along with the geometric and material symmetry with respect to the crack line, allows the crack surfaces to separate not in the opening mode, but in the sliding mode so that only the mode II thermoelastic deformation occurs (Choi, 2003). Furthermore, albeit the magnitudes of K_{II} in Fig. 6b decrease consistently as the crack angle θ increases, those of K_I in Fig. 6a reach their peak around the angle $\theta = 50°$. It should be remarked that comparison of the maximum values of K_I in Figs. 5a and 6a reveals that the heat flow in the direction of material gradation appears to give rise to the more severe near-tip condition than the vertical heat flow.

With the imposition of a fully insulated crack-surface condition ($\lambda_b = 0.0$) in the same material pair, Figs. 7 and 8 provide the variations of heat-flux intensity factors K_H as a function of θ when the heat flows in the horizontal and vertical directions, respectively, for different values of graded interlayer thickness, $h/2c$. In this case, the magnitude of K_H is shown to become larger as $h/2c$ increases with the implication that the interlayer of greater thickness is less effective in dissipating the heat in the near-tip region, which is seen to be considerable for the crack tip a.

The results in Figs. 9 and 10 illustrate the thermal-stress intensity factors that are associated with the thermal behavior in Figs. 7 and 8, respectively, over the given range of crack obliquity θ. It can

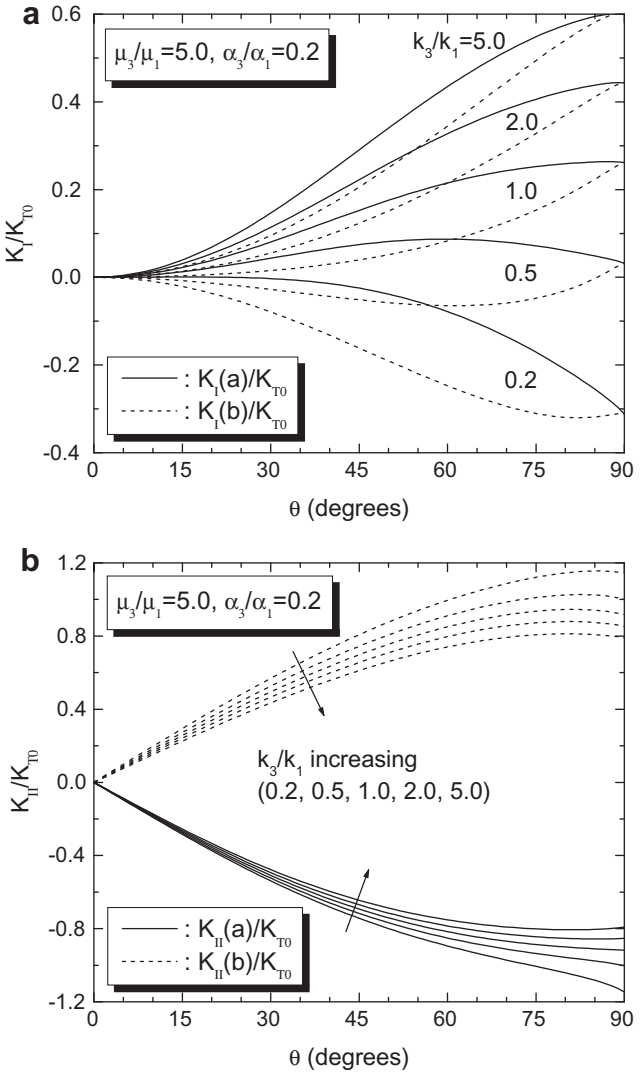

Fig. 15. Variations of thermal-stress intensity factors (a) K_I/K_{T0} and (b) K_{II}/K_{T0} as a function of θ under a horizontal heat flow $\left(\nabla T_x^\infty = \nabla T, \nabla T_y^\infty = 0\right)$ for different values of k_3/k_1 with $\mu_3/\mu_1 = 5.0$ and $\alpha_3/\alpha_1 = 0.2$ where $K_{T0} = 2\mu_1\alpha_1^*\nabla Tc^{3/2}/(1+\kappa)$, $\lambda_b = 0.0, h/2c = 0.5$, and $d/c = 0.0$.

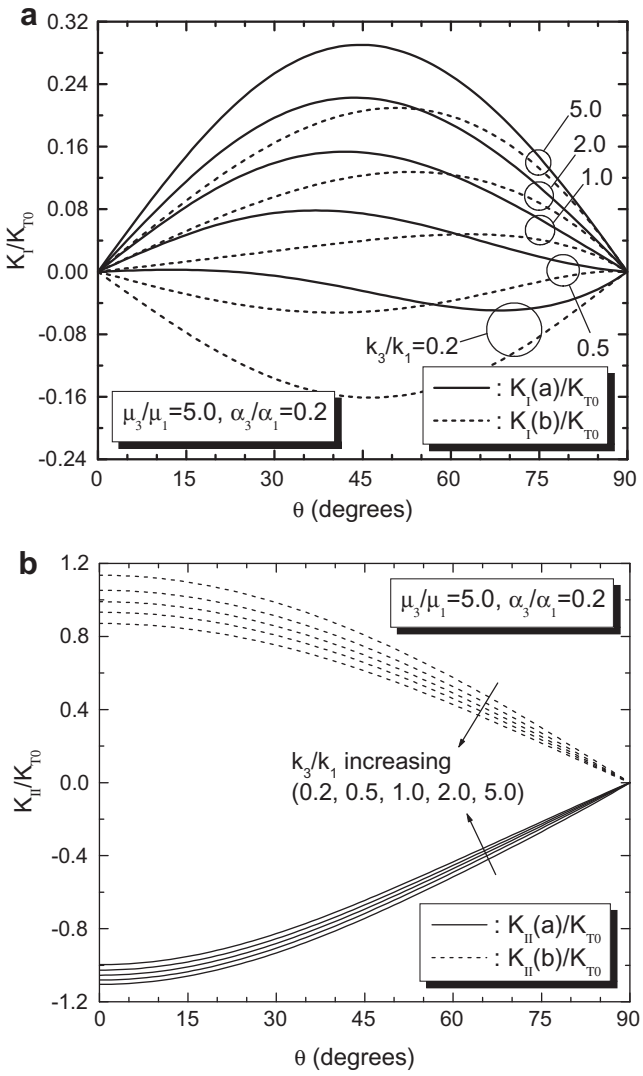

Fig. 16. Variations of thermal-stress intensity factors (a) K_I/K_{T0} and (b) K_{II}/K_{T0} as a function of θ under a vertical heat flow $\left(\nabla T_y^\infty = \nabla T, \nabla T_x^\infty = 0\right)$ for different values of k_3/k_1 with $\mu_3/\mu_1 = 5.0$ and $\alpha_3/\alpha_1 = 0.2$ where $K_{T0} = 2\mu_1\alpha_1^*\nabla Tc^{3/2}/(1+\kappa)$, $\lambda_b = 0.0, h/2c = 0.5$, and $d/c = 0.0$.

be depicted from Figs. 9a and 10a that the increase in the interlayer thickness $h/2c$ is likely to lower the magnitudes of K_I at both the crack tips, counteracting the effect of the nearby compliant constituent ($\mu_3/\mu_1 = 0.5658$). On the other hand, Figs. 9b and 10b clarify the crack-tip deformation that is compatible with the results in Figs. 7 and 8 such that the magnitudes of K_{II} become greater for the greater $h/2c$, which appears to be fairly noteworthy for the crack tip b. If the thickness of the graded interlayer were to increase even further relative to the crack size, the thermal-stress intensity factors in Figs. 9 and 10 which are now of mixed-mode would degenerate to those as plotted in Fig. 2, namely, the mode II thermal-stress intensity factors due to a uniform heat flow disturbed by a crack in the infinite homogeneous plane. To be noted is that locating the crack away from the interlayer ($d/c > 0.0$) would have a similar influence that is observed when increasing the interlayer thickness.

In the sequel, additional results are presented in Figs. 11–20 in order to examine the effects of material parameters ($k_3/k_1, \mu_3/\mu_1, \alpha_3/\alpha_1$) on the near-tip thermoelastic field as a function of crack orientation angle θ. It is assumed that $h/2c = 0.5$, $d/c = 0.0$, and $\lambda_b = 0.0$. To begin with, the results in Figs. 11 and 12 describe how the thermal conductivity ratio k_3/k_1 affects the thermal behavior under the horizontal and vertical heat flows, respectively. It is predicted that the magnitude of heat-flux intensity factors K_H is reduced as the ratio k_3/k_1 is increased, implying the enhanced thermal protection for the crack by the facilitated heat dissipation through the neighboring constituent that possesses the higher thermal conductivity.

The dependence of thermal-stress intensity factors on the thermoelastic parameters is next discussed for the prescribed range of crack obliquity θ. With the ratios of shear moduli and thermal expansion coefficients being fixed as (μ_3/μ_1, α_3/α_1) = (0.2, 0.2), the results are shown in Figs. 13 and 14 for different values of the thermal conductivity ratio k_3/k_1, when the heat flows in the horizontal and vertical directions, respectively. Specifically, those in Figs. 13a and 14a dictate that the increase in the ratio k_3/k_1 has a tendency to build up the severity of thermoelastic deformation in the opening mode, by amplifying substantially the values of K_I. On the other hand, in compliance with the thermal response in Figs. 11 and 12, one can observe from Figs. 13b and 14b that the increase in the

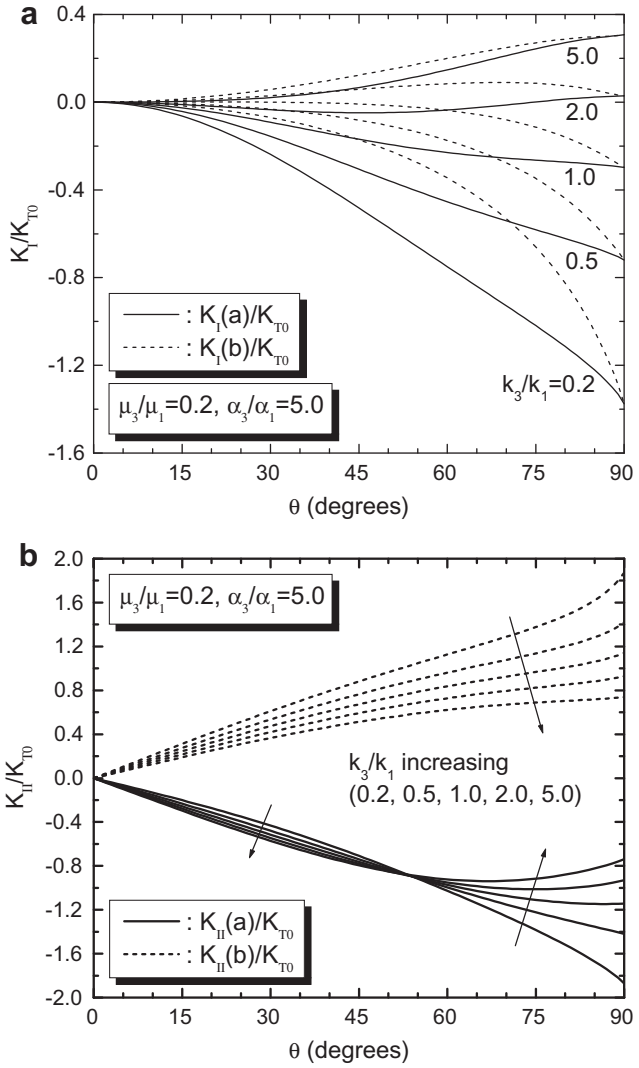

Fig. 17. Variations of thermal-stress intensity factors (a) K_I/K_{T0} and (b) K_{II}/K_{T0} as a function of θ under a horizontal heat flow $\left(\nabla T_x^\infty = \nabla T, \nabla T_y^\infty = 0\right)$ for different values of k_3/k_1 with $\mu_3/\mu_1 = 0.2$ and $\alpha_3/\alpha_1 = 5.0$ where $K_{T0} = 2\mu_1\alpha_1^*\nabla T c^{3/2}/(1+\kappa)$, $\lambda_b = 0.0, h/2c = 0.5$, and $d/c = 0.0$.

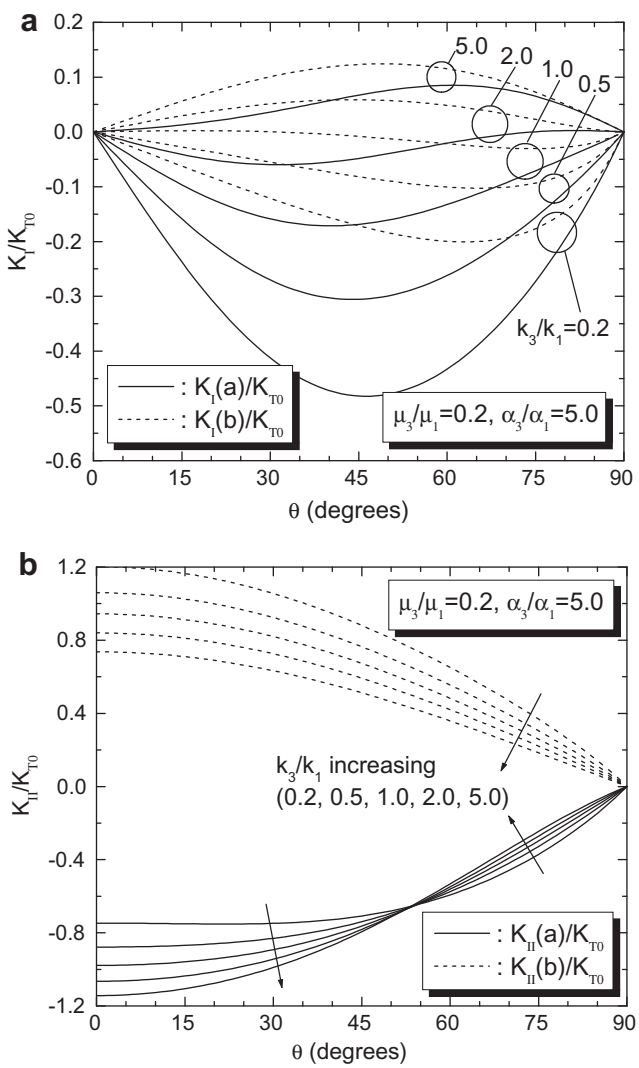

Fig. 18. Variations of thermal-stress intensity factors (a) K_I/K_{T0} and (b) K_{II}/K_{T0} as a function of θ under a vertical heat flow $\left(\nabla T_y^\infty = \nabla T, \nabla T_x^\infty = 0\right)$ for different values of k_3/k_1 with $\mu_3/\mu_1 = 0.2$ and $\alpha_3/\alpha_1 = 5.0$ where $K_{T0} = 2\mu_1\alpha_1^*\nabla T c^{3/2}/(1+\kappa)$, $\lambda_b = 0.0, h/2c = 0.5$, and $d/c = 0.0$.

ratio k_3/k_1 tends to attenuate the thermoelastic singular behavior in the shear mode.

For the combination of thermoelastic properties as $(\mu_3/\mu_1, \alpha_3/\alpha_1) = (5.0, 0.2)$, the corresponding thermal-stress intensity factors due to the horizontal and vertical heat flows are presented in Figs. 15 and 16, respectively. Of interest in this case is the crack closure as can commonly be exemplified by the negative values of K_I in both Figs. 15a and 16a, which are obtained when $k_3/k_1 < 1.0$ in conjunction with the rigid constraint from the adjoining stiffer constituent as $\mu_3/\mu_1 = 5.0$. The variations of K_{II} with respect to the crack obliquity θ and the ratio k_3/k_1 in Figs. 15b and 16b, however, remain analogous to those in Figs. 13b and 14b.

As demonstrated in Fig. 17a and 18a for the values of K_I obtained under the heat flow in the horizontal and vertical directions, respectively, the increase in the thermal expansion coefficient as $(\mu_3/\mu_1, \alpha_3/\alpha_1) = (0.2, 5.0)$ also enforces such crack closing behavior to prevail in an obvious manner in the range of θ. This trend is shown to become more notable if the thermal conductivity of the adjacent constituent is lowered relative to that of the cracked constituent. Moreover, the results in Figs. 17b and 18b indicate that the effect of the ratio k_3/k_1 on the values of K_{II} at the crack tip a is reflected differently, depending on the crack orientation angle θ.

The variations of thermal-stress intensity factors for the material pair, $(\mu_3/\mu_1, \alpha_3/\alpha_1) = (5.0, 5.0)$, are provided in Figs. 19 and 20 as a function of θ for the horizontal and vertical heat flows, respectively. It is then remarkable that the values of K_I are obtained to be all negative for the given thermal conductivity ratios k_3/k_1, as plotted in Figs. 19a and 20a, causing the crack surfaces to be rather firmly closed with the greater magnitudes of K_I. Such crack closure is predicted to be even more pronounced for the interfacial crack ($\theta = 90^o$) under the horizontal heat flow and for the oblique crack ($\theta \cong 50°$) subjected to the vertical heat flow, especially when the ratio k_3/k_1 is smaller than unity. As can be observed in Figs. 19b and 20b, the values of K_{II} delineate the quite intricate near-tip thermoelastic behavior, marking another salient departure from those in Figs. 13b–16b. It should now be pointed out that the thermal-stress intensity factors of the oblique crack appear to be more strongly affected by the variation of thermal conductivity coefficients when the adjoining constituent retains the stiffer modulus

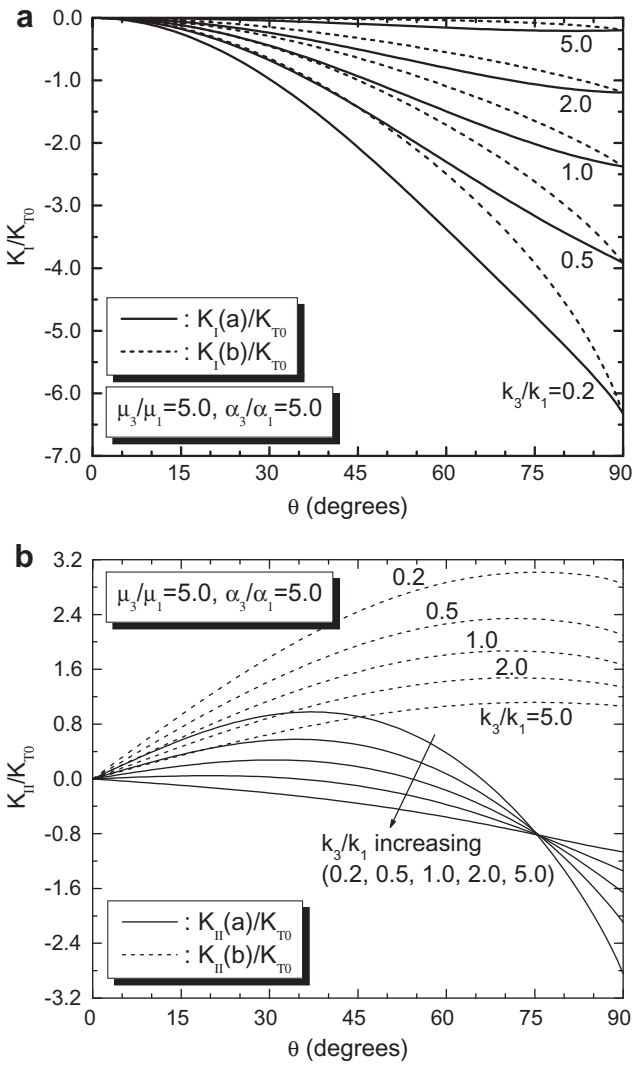

Fig. 19. Variations of thermal-stress intensity factors (a) K_I/K_{T0} and (b) K_{II}/K_{T0} as a function of θ under a horizontal heat flow $\left(\nabla T_x^\infty = \nabla T, \nabla T_y^\infty = 0\right)$ for different values of k_3/k_1 with $\mu_3/\mu_1 = 5.0$ and $\alpha_3/\alpha_1 = 5.0$ where $K_{T0} = 2\mu_1\alpha_1^*\nabla T c^{3/2}/(1+\kappa)$, $\lambda_b = 0.0, h/2c = 0.5$, and $d/c = 0.0$.

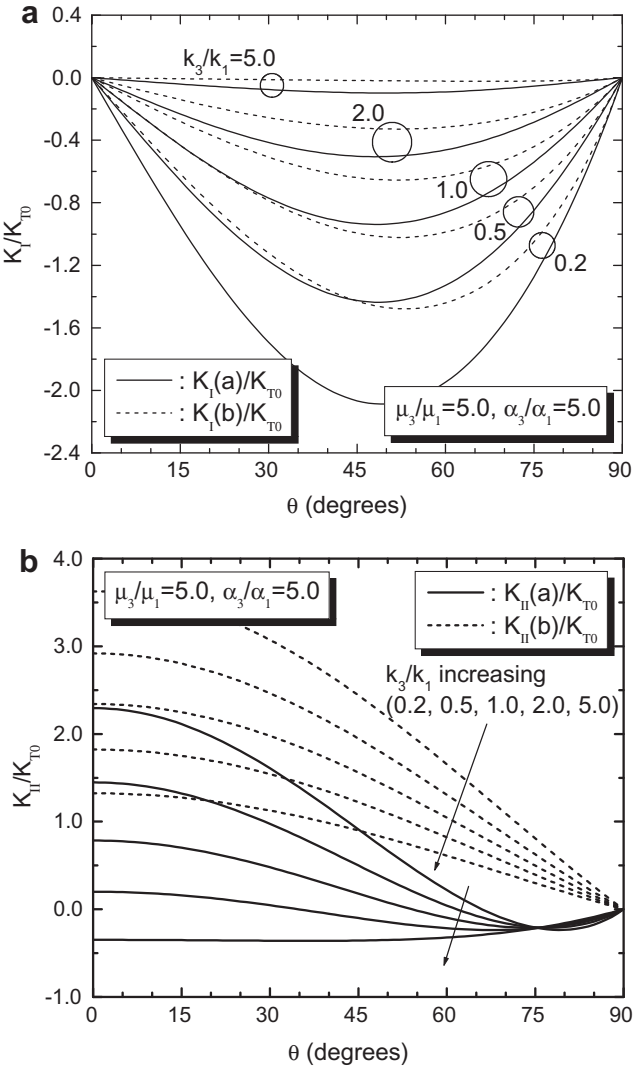

Fig. 20. Variations of thermal-stress intensity factors (a) K_I/K_{T0} and (b) K_{II}/K_{T0} as a function of θ under a vertical heat flow $\left(\nabla T_y^\infty = \nabla T, \nabla T_x^\infty\right) = 0$ for different values of k_3/k_1 with $\mu_3/\mu_1 = 5.0$ and $\alpha_3/\alpha_1 = 5.0$ where $K_{T0} = 2\mu_1\alpha_1^*\nabla T c^{3/2}/(1+\kappa)$, $\lambda_b = 0.0, h/2c = 0.5$, and $d/c = 0.0$.

along with the greater thermal expansion coefficient. Throughout the results in Figs. 13–20, it can thereby be conjectured that for the oblique crack geometry, the thermal-stress intensity factors under the horizontal heat flow are induced to be of greater magnitude when compared with those due to the vertical heat flow, which is particularly true for the stress intensification in the opening mode.

7. Closure

The thermoelastic problem of uniform steady-state heat flows disturbed by a partially insulated crack at an arbitrary angle to the graded interfacial zone in bonded media has been investigated. Based on the use of plane thermoelasticity equations and the method of Fourier integral transform, two sets of singular integral equations were derived for heat conduction and thermal stresses. The emphasis was placed on the quantification of thermoelastic deformation in the near-tip region in terms of the values of heat-flux and thermal-stress intensity factors that elaborated several unique and salient features in response to the variations of thermophysical parameters in the problem over the given range of crack orientation angle. The very involved nature of the crack-tip behavior was indicated under the current nonisothermal loading environment, which is quite distinctive from that previously observed under the isothermal counterpart.

Specifically, it was manifested that the singular thermal stress field around the crack tends to be intensified to a larger extent by the horizontal heat flow in the direction of material gradation than the heat flow in the vertical direction. It was also noteworthy that when the neighboring uncracked constituent possesses the stiffness and thermal expansion that are greater than those of the cracked one, but with the lowered thermal conductivity, the oblique crack in the bonded system has the enhanced likelihood of being closed, as could be inferred by the negative mode I thermal-stress intensity factors, with the implication of the ensuing possibility of crack-surface contact and friction. Although the traction-free crack surface condition is thus invalidated, the contact and friction between the closed crack surfaces were not taken into account in the present work, in the sense that the crack closure is what may take place in reality under the influence of prescribed thermal loading and the corresponding negative values of mode I stress intensification could still be applicable, if the superposition with those due to the large enough residual and/or other tensile loading gives rise to the positive resultants and keeps the crack open.

In the mixed-mode thermal crack problem presented herein, another point of interest would be to assess the possible crack growth and arrest process based on the appropriate fracture criterion. Whether the further crack extension would be the cleavage of the adjacent graded interlayer, debonding along the nominal interface or reflection back into the substrate may depend on the relative toughness to load factor ratios. Together with the values of stress intensity factors, this basically requires the resources regarding the material resistance to fracture in the near-tip region, especially when the crack intersects or lies along the interface with the interlayer that essentially exhibits the nonhomogeneous variation in its fracture toughness. Such consideration is, however, beyond the scope of the current study and is left for the future investigation.

Acknowledgements

This work has been conducted by the faculty research program 2008 of Kookmin University, Seoul 136-702, Republic of Korea. The support is gratefully acknowledged.

Appendix A

The arbitrary unknowns, $A(s)$, $B_j(s)$, $j = 1, 2$, and $C(s)$, in the general solutions for the temperature field are obtained in terms of the auxiliary function ϕ_0 as:

$$A(s) = \frac{(\lambda_1 - |s|)(\lambda_2 - |s|)(e^{-\lambda_1 h} - e^{-\lambda_2 h})}{2s\Delta_0(s)} I_0(s) \tag{A.1}$$

$$B_1(s) = \frac{|s|(\lambda_2 - |s|)e^{-\lambda_2 h}}{s\Delta_0(s)} I_0(s) \tag{A.2}$$

$$B_2(s) = -\frac{|s|(\lambda_1 - |s|)e^{-\lambda_1 h}}{s\Delta_0(s)} I_0(s) \tag{A.3}$$

$$C(s) = \frac{|s|(\lambda_2 - \lambda_1)e^{-(\lambda_1+\lambda_2-|s|)h}}{s\Delta_0(s)} I_0(s) \tag{A.4}$$

where $\Delta_0(s)$ and $I_0(s)$ are given by

$$\Delta_0(s) = (\lambda_1 + |s|)(\lambda_2 - |s|)e^{-\lambda_2 h} - (\lambda_1 - |s|)(\lambda_2 + |s|)e^{-\lambda_1 h} \tag{A.5}$$

$$I_0(s) = i\int_a^b \phi_0(t) e^{-m|s|t+inst} dt \tag{A.6}$$

Appendix B

The elements of a vector $\Psi(s) = \{\Psi_1(s), \Psi_2(s), \Psi_3(s), \Psi_4(s)\}^T$ in Eq. (44a) are expressed in terms of the auxiliary functions ϕ_0 and ϕ_j, $j = 1, 2$, as:

$$\begin{aligned}\Psi_1(s) &= -\frac{2\alpha_1^*}{1+\kappa}\int_a^b \phi_0(t)\left[\frac{imn}{s^2} + \frac{1}{2s}\left(\frac{m^2-n^2}{|s|} + mt\right)\right] e^{-m|s|t+inst} dt \\ &+ \frac{1}{1+\kappa}\int_a^b \phi_1(t)\left[im\left(\frac{1-\kappa}{2|s|} - mt\right) - n\left(\frac{1+\kappa}{2s} + \frac{s}{|s|}mt\right)\right] e^{-m|s|t+inst} dt \\ &+ \frac{1}{1+\kappa}\int_a^b \phi_2(t)\left[in\left(\frac{1-\kappa}{2|s|} - mt\right) + m\left(\frac{1+\kappa}{2s} + \frac{s}{|s|}mt\right)\right] e^{-m|s|t+inst} dt\end{aligned} \tag{B.1}$$

$$\begin{aligned}\Psi_2(s) &= -\frac{2\alpha_1^*}{1+\kappa}\int_a^b \phi_0(t)\left[\frac{imn}{s|s|} + m\left(\frac{m}{s^2} + \frac{t}{2|s|}\right)\right] e^{-m|s|t+inst} dt \\ &+ \frac{1}{1+\kappa}\int_a^b \phi_1(t)\left[im\left(\frac{1+\kappa}{2s} - \frac{s}{|s|}mt\right) - n\left(\frac{1-\kappa}{2|s|} + mt\right)\right] e^{-m|s|t+inst} dt \\ &+ \frac{1}{1+\kappa}\int_a^b \phi_2(t)\left[in\left(\frac{1+\kappa}{2s} - \frac{s}{|s|}mt\right) + m\left(\frac{1-\kappa}{2|s|} + mt\right)\right] e^{-m|s|t+inst} dt\end{aligned} \tag{B.2}$$

$$\begin{aligned}\Psi_3(s) &= -\frac{4\mu_1\alpha_1^*}{1+\kappa}\int_a^b \phi_0(t)\left[\frac{imn}{|s|} + m\left(\frac{m}{s} + \frac{s}{|s|}\frac{t}{2}\right)\right] e^{-m|s|t+inst} dt \\ &- \frac{2\mu_1}{1+\kappa}\int_a^b \phi_1(t)\left[im^2|s|t + n\frac{s}{|s|}(1 + m|s|t)\right] e^{-m|s|t+inst} dt \\ &- \frac{2\mu_1}{1+\kappa}\int_a^b \phi_2(t)\left[imn|s|t - m\frac{s}{|s|}(1 + m|s|t)\right] e^{-m|s|t+inst} dt\end{aligned} \tag{B.3}$$

$$\begin{aligned}\Psi_4(s) &= -\frac{4\mu_1\alpha_1^*}{1+\kappa}\int_a^b \phi_0(t)\left[\frac{imn}{s} + \frac{1}{2}\left(\frac{m^2-n^2}{|s|} + mt\right)\right] e^{-m|s|t+inst} dt \\ &+ \frac{2\mu_1}{1+\kappa}\int_a^b \phi_1(t)\left[im\frac{s}{|s|}(1 - m|s|t) - mn|s|t\right] e^{-m|s|t+inst} dt \\ &+ \frac{2\mu_1}{1+\kappa}\int_a^b \phi_2(t)\left[in\frac{s}{|s|}(1 - m|s|t) + m^2|s|t\right] e^{-m|s|t+inst} dt\end{aligned} \tag{B.4}$$

References

Bahar, L.Y., 1972. Transfer matrix approach to layered system. ASCE Journal of Engineering Mechanics 98, 1159–1172.

Barber, J.R., 1976. The disturbance of a uniform steady-state heat flux by a partially conducting plane crack. International Journal of Heat and Mass Transfer 19, 956–958.

Barber, J.R., 1980. Steady-state thermal stresses caused by an imperfectly conducting penny-shaped crack in an elastic solid. Journal of Thermal Stresses 3, 77–83.

Chan, Y.-S., Paulino, G.H., Fannjiang, A.C., 2008. Gradient elasticity theory for mode III fracture in functionally graded materials – Part II: Crack parallel to the material gradation. ASME Journal of Applied Mechanics 75, 061015.

Chen, J., 2005. Determination of thermal stress intensity factors for an interface crack in a graded orthotropic coating-substrate structure. International Journal of Fracture 133, 303–328.

Choi, H.J., 1996. Bonded dissimilar strips with a crack perpendicular to the functionally graded interface. International Journal of Solids and Structures 33, 4101–4117.

Choi, H.J., 1997. A periodic array of cracks in a functionally graded nonhomogeneous medium loaded under in-plane normal and shear. International Journal of Fracture 88, 107–128.

Choi, H.J., 2001a. The problem for bonded half-planes containing a crack at an arbitrary angle to the graded interfacial zone. International Journal of Solids and Structures 38, 6559–6588.

Choi, H.J., 2001b. Effects of graded layering on the tip behavior of a vertical crack in a substrate under frictional Hertzian contact. Engineering Fracture Mechanics 68, 1033–1059.

Choi, H.J., 2003. Thermoelastic problem of steady-state heat flow disturbed by a crack perpendicular to the graded interfacial zone in bonded materials. Journal of Thermal Stresses 26, 997–1030.

Choi, H.J., 2004. Impact response of a surface crack in a coating/substrate system with a functionally graded interlayer: antiplane deformation. International Journal of Solids and Structures 41, 5631–5645.

Choi, H.J., 2006. Elastodynamic analysis of a crack at an arbitrary angle to the graded interfacial zone in bonded half-planes under antiplane shear impact. Mechanics Research Communications 33, 636–650.

Choi, H.J., 2007a. Stress intensity factors for an oblique edge crack in a coating/substrate system with a graded interfacial zone under antiplane shear. European Journal of Mechanics-A/Solids 26, 337–347.

Choi, H.J., 2007b. Impact behavior of an inclined edge crack in a layered medium with a graded nonhomogeneous interfacial zone: antiplane deformation. Acta Mechanica 193, 67–84.

Choi, H.J., Jin, T.E., Lee, K.Y., 1998. Collinear cracks in a layered half-plane with a graded nonhomogeneous interfacial zone – Part II: Thermal shock response. International Journal Fracture 94, 123–135.

Choi, H.J., Paulino, G.H., 2010. Interfacial cracking in a graded coating/substrate system loaded by a frictional sliding flat punch. Proceedings of the Royal Society A: Mathematical, Physical and Engineering Sciences 466, 853–880.

Dag, S., Erdogan, F., 2002. A surface crack in a graded medium loaded by a sliding rigid stamp. Engineering Fracture Mechanics 69, 1729–1751.

Dag, S., Yildirim, B., 2009. Computation of thermal fracture parameters for inclined cracks in functionally graded materials using J_k-integral. Journal of Thermal Stresses 32, 530–556.

Davis, P.J., Rabinowitz, P., 1984. Methods of Numerical Integration, second ed. Academic Press, New York.

Eischen, J.W., 1987. Fracture of nonhomogeneous materials. International Journal of Fracture 34, 3–22.

El-Borgi, S., Erdogan, F., Hatira, F.B., 2003. Stress intensity factors for an interface crack between a functionally graded coating and a homogeneous substrate. International Journal of Fracture 123, 139–162.

El-Borgi, S., Hidri, L., Abdelmoula, R., 2006. An embedded crack in a graded coating bonded to a homogeneous substrate under thermo-mechanical loading. Journal of Thermal Stresses 29, 439–466.

Erdogan, F., 1978. Mixed boundary value problems in mechanics. In: Nemat-Nasser, S. (Ed.), Mechanics Today, vol. 4. Pergamon Press, New York, pp. 1–86.

Erdogan, F., 1998. Crack problems in nonhomogeneous materials. In: Cherepanov, G.P. (Ed.), Fracture, A Topical Encyclopedia of Current Knowledge. Krieger, Malabar, pp. 72–98.

Erdogan, F., Wu, B.H., 1996. Crack problems in FGM layers under thermal stresses. Journal of Thermal Stresses 19, 237–265.

Fujimoto, T., Noda, N., 2001. Influence of the compositional profile of functionally graded material on the crack path under thermal shock. Journal of the American Ceramic Society 84, 1480–1486.

Gharbi, M., El-Borgi, S., Chafra, M., 2009. A surface crack in a graded coating bonded to a homogeneous substrate under transient thermal loading. Journal of Thermal Stresses 32, 394–413.

Gradshteyn, I.S., Ryzhik, I.M., 2000. Table of Integrals, Series, and Products, sixth ed. Academic Press, New York.

Huang, G.-Y., Wang, Y.-S., Yu, S.-W., 2004. A new model of functionally graded coatings with a crack under thermal loading. Journal of Thermal Stresses 27, 491–512.

Itou, S., 2004. Thermal stresses around a crack in the nonhomogeneous interfacial layer between two dissimilar elastic half-planes. International Journal of Solids and Structures 41, 923–945.

Jin, Z.-H., Batra, R.C., 1996. Stress intensity relaxation at the tip of an edge crack in a functionally graded material subjected to a thermal shock. Journal of Thermal Stresses 19, 317–339.

Jin, Z.-H., Noda, N., 1994a. Crack-tip singular fields in nonhomogeneous materials. ASME Journal of Applied Mechanics 61, 738–740.

Jin, Z.-H., Noda, N., 1994b. Transient thermal stress intensity factors for a crack in a semi-infinite plate of a functionally gradient material. International Journal of Solids and Structures 31, 203–218.

Kim, J.-H., Amit, K.C., 2008. A generalized interaction integral method for the evaluation of the T-stress in orthotropic functionally graded materials under thermal loading. ASME Journal of Applied Mechanics 75, 051112.

Lee, H.-J., Choi, H.J., 2006. Effects of graded properties on the impact response of an interface crack in a coating/substrate system subjected to antiplane deformation. Zeitschrift für Angewandte Mathematik und Mechanik 86, 110–119.

Long, X., Delale, F., 2005. The mixed mode crack problem in an FGM layer bonded to a homogeneous half-plane. International Journal of Solids and Structures 42, 3897–3917.

Miyamoto, Y., Kaysser, W.A., Rabin, B.H., Kawasaki, A., Ford, R.G. (Eds.), 1999. Functionally Graded Materials: Design, Processing, and Applications. Kluwer Academic Publishers, MA.

Muskhelishvili, N.I., 1953. Singular Integral Equations. Noordhoff, The Netherlands.

Noda, N., Jin, Z.-H., 1993. Thermal stress intensity factors for a crack in a strip of a functionally gradient material. International Journal of Solids and Structures 30, 1039–1056.

Nowinski, J.L., 1978. Theory of Thermoelasticity with Applications. Sijthoff & Noordhoff, The Netherlands.

Paulino, G.H., Fannjiang, A.C., Chan, Y.-S., 2003. Gradient elasticity theory for mode III fracture in functionally graded materials – Part I: Crack perpendicular to the material gradation. ASME Journal of Applied Mechanics 70, 531–542.

Rice, J.R., 1988. Elastic fracture mechanics concepts for interfacial cracks. ASME Journal of Applied Mechanics 55, 98–103.

Romeo, A., Ballarini, R., 1995. A crack very close to a bimaterial interface. ASME Journal of Applied Mechanics 62, 614–619.

Schulz, U., Peters, M., Bach, Fr.-W., Tegeder, G., 2003. Graded coatings for thermal, wear and corrosion barriers. Materials Science and Engineering A362, 61–80.

Sekine, H., 1987. Thermal stress singularities. In: Hetnarski, R.B. (Ed.), Thermal Stresses II. Elsevier Science Publishers, New York, pp. 57–117.

Sih, G.C., 1965. Heat conduction in the infinite medium with lines of discontinuities. ASME Journal of Heat Transfer 87, 293–298.

Tzou, D.Y., 1991. The singular behavior of the temperature gradient in the vicinity of a macrocrack tip. International Journal of Heat and Mass Transfer 33, 2625–2630.

Walters, M.C., Paulino, G.H., Dodds Jr., R.H., 2004. Stress-intensity factors for surface cracks in functionally graded materials under mode-I thermomechanical loading. International Journal of Solids and Structures 41, 1081–1118.

Yildirim, B., 2006. An equivalent domain integral method for fracture analysis of functionally graded materials under thermal stresses. Journal of Thermal Stresses 29, 371–397.

Zhou, Y., Li, X., Yu, D., 2010. A partially insulated interface crack between a graded orthotropic coating and a homogeneous orthotropic substrate under heat flux supply. International Journal of Solids and Structures 47, 768–778.